AN EXPERIMENTAL INVESTIGATION OF ELECTROMECHANICAL RESPONSE IN POLYURETHANE ELASTOMER (DOW 2103-80AE)

Period 1 July 1995 to 30 July 1997

Final Report

OFFICE OF NAVAL RESEARCH
Contract No.: N00014-95-1-1225

Qiming Zhang

REPORT DOCUMENTATION PAGE

Form Approved
OMB No. 0704-0188

1. AGENCY USE ONLY (Leave blank)	2. REPORT DATE	3. REPORT TYPE AND DATES COVERED
	1 August 1997	Final Technical Report 07/01/95-07/30/97

4. TITLE AND SUBTITLE
An Experimental Investigation of Electromechanical Response in Polyurethane Elastomer (Dow 2103-80AE)

5. FUNDING NUMBERS
N00014-95-1-1225

6. AUTHOR(S)
Qiming Zhang

7. PERFORMING ORGANIZATION NAME(S) AND ADDRESS(ES)
Materials Research Laboratory
Electrical Engineering Department
The Pennsylvania State University
University Park, PA 16802

8. PERFORMING ORGANIZATION REPORT NUMBER

9. SPONSORING/MONITORING AGENCY NAME(S) AND ADDRESS(ES)
Wallace A. Smith
Office of Naval Research, ONR 332
Ballston Tower One
800 North Quincy Street
Arlington, VA 22217-5660

10. SPONSORING/MONITORING AGENCY REPORT NUMBER

11. SUPPLEMENTARY NOTES

12a. DISTRIBUTION/AVAILABILITY STATEMENT
Distribution is unlimited

12b. DISTRIBUTION CODE

13. ABSTRACT *(Maximum 200 words)*

In this program, the electric field induced strain response and other related material properties for the polyurethane elastomer (Dow 2103-80AE), which was reported to exhibit a giant strain response, were investigated. We show that the observed large field induced strain is only a thin film effect and in bulk samples, the electromechanical response is not significant. To understand how various effects influence the electromechanical response in this type of material, we examined the material properties in both bulk samples and thin films. In bulk samples, we show that the polymer chain segment motions can be divided into those responsible for the mechanical, those for the polarization (dielectric), and those for both (electromechanical). By molecular engineering, one should be able to selectively enhance different type of the chain segment motions for different applications. Although a great deal of efforts have been devoted to the characterization of the field induced strain response in thin and soft samples, there was no existing device which is capable of measuring the strain in thin polymer samples reliably and conveniently. To overcome this difficult, a novel bimorph based dilatometer was developed for the strain measurement in thin and soft polymer films, which exhibits a high resolution, reliability, and great convenience. Based on the experimental results on thin films samples, we conclude that the space charge injection, which results in a non-uniform charge distribution and hence, a non-uniform electric field distribution across the sample thickness, is responsible for the large field induced strain response observed in thin film samples.

14. SUBJECT TERMS

15. NUMBER OF PAGES

16. PRICE CODE

17. SECURITY CLASSIFICATION OF REPORT	18. SECURITY CLASSIFICATION OF THIS PAGE	19. SECURITY CLASSIFICATION OF ABSTRACT	20. LIMITATION OF ABSTRACT
UNCLASSIFIED	UNCLASSIFIED	UNCLASSIFIED	UNLIMITED

I. Introduction

Electromechanical coupling effects such as piezoelectricity and electrostriction have been widely utilized in many areas such as transducers and sensors.[1,2] Conventional electromechanical transduction materials include ceramics such as lead zirconate titanate (PZT) and lead magnesium niobate-lead titanate (PMN-PT) and single crystals such as quartz.[1,3] During the last three decades, electromechanical polymers have drawn much attention because they have high mechanical flexibility, low acoustic impedance, low manufacturing cost, and can be easily molded into desirable shapes.[4,5] However, the low electromechanical activity of the polymeric materials greatly limits their applications. For instance, the electromechanical coupling factor of the piezoelectric polyvinylidene fluoride (PVDF) and its copolymers with trifluoroethylene (TrFE), which possess the highest electromechanical activity among all the known electromechanical polymers, is less than 0.25.[6] In contrast, piezoceramic PZT has a coupling factor of 0.75.[3] Considering the fact that the energy conversion efficiency is proportional to the square of the coupling factor, the difference between the two is quite significant. Hence, there is constant searching for new polymeric materials with high electromechanical activity. Recently, it was reported that in certain polyurethane elastomers (for example, Dow 2103-80AE), a large electric field induced strain can be achieved and in the electric field biased state, the materials exhibit an effective piezoelectric coefficient higher than those of piezoceramic PZTs, which have stirred much excitement and interest in this class of materials.[7]

Since the discovery of this new class of materials, many experimental investigations have been conducted. It has been shown that the characteristics of the polarization response to applied electric fields indicate that the material is not a ferroelectric and the strain is proportional to the square of the applied electric field, in analogy to the electrostrictive effect.[6,7] Because of these

features and the high elastic compliance of the material, which is in the range between 10^{-7} and 10^{-8} m^2/N, the question of whether the large electric field induced strain is caused by the Maxwell stress effect, i.e., the Coulomb interaction between the charges on the two electrodes of the specimen, is often raised. In fact, the Coulomb attraction between the charges on the two electrodes has been widely utilized to produce actuators and transducers such as those in the current Microelectro-Mechanical Systems.[8] This possibility is reinforced by a recent experimental result which indicates that by increasing the elastic compliance of the polyurethane, the field induced strain was enhanced.[6]

The objective of this investigation is to provide an understanding of the possible mechanism for the observed large electric field induced strain in this class of polyurethane elastomers. Through this process, we also intend to examine the nature or general features of electromechanical responses in non-ferroelectric polymeric materials. Although the dielectric and elastic responses of polymeric materials have been investigated for many decades both experimentally and theoretically and are relatively well understood,[9] the investigation on the electromechanical response in polymeric materials, except those of piezoelectricity in PVDF and its copolymers, is much less extensive and consequently, the understanding on the elastoelectric properties of polymers is relatively poor .

Through this investigation, it was found that the electric field induced strain is very sensitive to the sample processing conditions and the thickness of the specimen. The field induced strain by an unit external electric field increases as the film thickness is reduced. In fact, in this type of polyurethane material the electric field induced strain response in thick samples is not significant at all. We suggest that the enhanced strain response in thin film samples be caused by a non-uniform electric field distribution across the thickness direction in the samples since for a strain response proportional to the square of the applied electric field, any non-uniform field distribution in a sample will increase the strain response. The most probable cause for such a

thickness dependence behavior is the existence of a surface region and an interior region, which have different electric field strength, in a specimen, and could be a result of charge injection and/or a non-uniform distribution of the material properties, as schematically drawn in figure 1(a).[6,10]

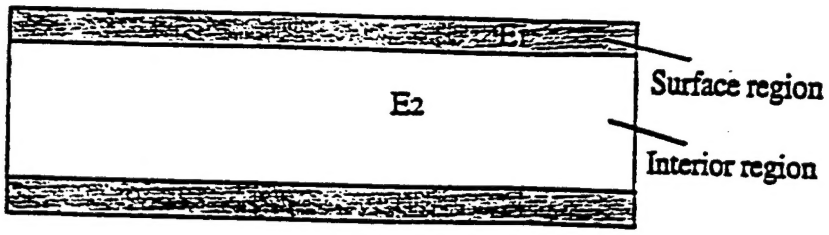

(a)

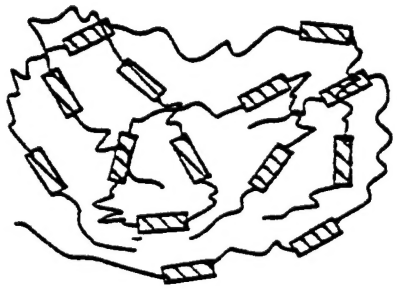

(b)

FIG. 1. (a) Schematical drawing of a polyurethane sample showing the surface region (hatched regions) and interior region. The electric fields E_1 and E_2 in the two regions may not be the same. (b) Schematic of the morphology of a polyurethane elastomer where the hard segments (hatched boxes) are embedded in the matrix of soft segments (thin lines).

In this investigation, we first examined the electromechanical properties of thick samples in which the interface effect can be neglected and the properties measured reflect the bulk response

of the materials. We found that in the polyurethane elastomers, there are two groups of the segment motions: those generate dielectric response and those generate the mechanical response. These two groups will overlap which is responsible for the electromechanical response in the material. This result is significant since it points out the possibility of change the ratio between the two groups to enhance one property over the other. We plan to carry out a more detailed study in this direction. Through this investigation, we also identified the contribution of the Maxwell stress effect to the total strain response.

Although a great deal of efforts have been devoted to the characterization of the electric field induced strain response in thin soft polymer films, no-one of the existing techniques can perform the measurement reliably and conveniently. In order to address this issue, we investigated several approaches and based on the results, we developed a novel bimorph based dilatometer. As will be shown in this report, the device can provide an accurate measurement on the strain response in thin and soft polymer samples and it is quite convenient to use.

Making use of this newly developed dilatometer, we systematically investigated the electric field induced strain response in thin polyurethane films over a broad frequency range. From this study, we show that the homo-charge injection is responsible for the built-up of the non-uniform charge distribution which results in a non-uniform electric field distribution across the thickness direction.

Hence, in the section II, the results on bulk samples are reported. In the section III, the details of the newly developed bimorph based dilatometer are described. In the section IV, we report on the results on thin films and demonstrate that the homo-charge injection is responsible for the enhanced electric field induced strain observed in thin films. In the section V, a brief summary of the results and some of the future plans will be made.

II. Electromechanical response in thick polyurethane elastomer samples:

2.1. Experimental

The polyurethane used in this investigation is produced by Deerfield Urethane, Inc. using a Dow polyurethane (Dow 2103-80AE). The sample was cast and the thickness of the sample is 2 mm. As will be shown later, for a sample of such a thickness, the effect of surface regions in causing a non-uniform electric field distribution in the specimen is not significant and the observed response can be regarded as from a bulk material with approximately a uniform electric field distribution across the sample thickness direction.

Polyurethane elastomer is a block copolymer with hard segments embedded in a soft segment matrix as schematically drawn in figure 1(b).[11] For the polymer investigated, the soft segment is poly(tetramethylene glycol) (PTMEG) with molecular weight of about 1000. The hard segment is comprised of a diisocyanate and a diol chain extender. The diisocyanate is methylenedi-p-phenyl diisocyanate (MDI) and the diol chain extender is 1,4-butanediol (BD). The mole ratio of the components is about

1.8 mol MDI / 0.8 mol BD / 1.0 mol PTMEG.

Hence, the hard segment (MDI + BD) is approximately 34% by weight in the sample.

The x-ray scattering result, shown in figure 2, reveals that both the hard segment and soft segment are in the amorphous phase and there is no detectable crystalline phase in the material within the experiment resolution.

In this investigation, the dielectric constant, the elastic compliance, and the electric field induced strain were characterized over a wide temperature and frequency range. In addition, FTIR was also investigated over a wide temperature range to identify the changes in the transition region above the glass transition temperature.

The dielectric constant measurement was carried out by a HP LCR multimeter (HP 4274A), a HP impedance analyzer (HP 4192A), a capacitance bridge (General Radio 1616), and a lock-in amplifier (SR 850) depending on the capacitance value of the sample and the frequency range.

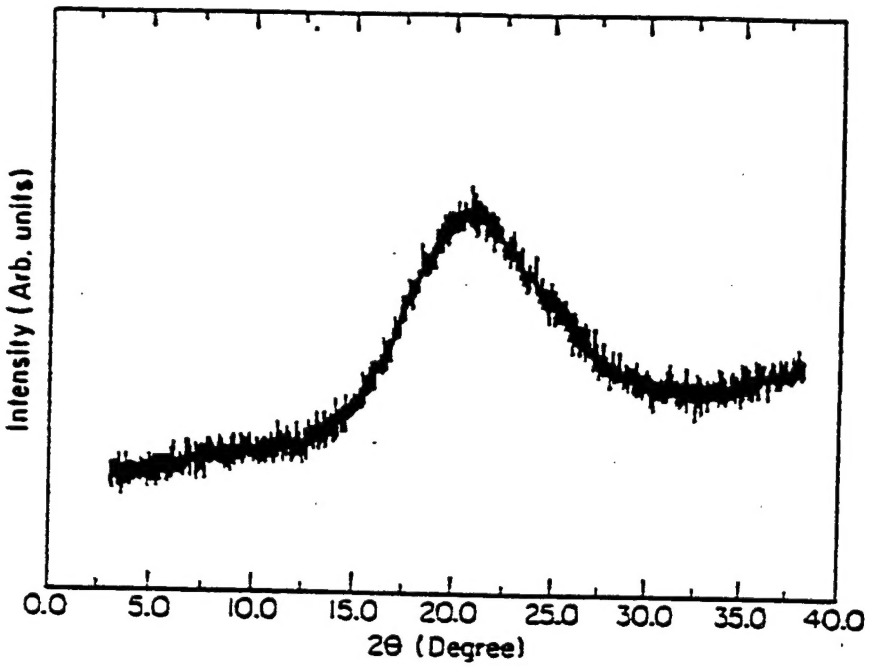

FIG. 2. X-ray diffraction data of the polyurethane elastomer at room temperature where the broad peak near 20° is the amorphous hola. No crystalline phase can be detected within the data resolution.

The lock-in amplifier, which measures both the phase and amplitude of the voltage and current applied to the specimen, yielding the impedance and the capacitance of the specimen, was used in the frequency range from 1 mHz to 1 kHz. The capacitance bridge covers the frequency range from 100 Hz to 100 kHz, HP LCR meter in the frequency range from 1 kHz to 1 MHz, and HP impedance analyzer in frequency from 1 kHz to 10 MHz. For the specimens with a capacitance value below 100 pF, the capacitance bridge was utilized since the error from LCR meter and impedance analyzer is quite large in measuring capacitance of small value. The temperature control was provided by a Delta chamber interfaced with a HP computer.

The electric field induced strain measurement for the thick samples was conducted by a double beam laser dilatometer which is equipped with a temperature chamber in the temperature range from -100 °C to about 200 °C.[12] The operating frequency range for the dilatometer is from 1 Hz to above 1 MHz. For the polymer specimens investigated, it was found that the spurious

resonance existing at high frequencies made it difficult to carry out measurements to frequencies above 10 kHz.

The elastic modulus was measured by a dynamic mechanical analysis system which covers a wide frequency and temperature range.

A Perkin-Elmer DSC-7 was employed to obtain the DSC curves and a Digilab Model FTS-45 at a resolution of 2 cm^{-1} was used to acquire the FTIR spectra for which a minimum of 64 scans were signal-averaged. The film used for FTIR examination was sufficiently thin to be within an absorbance range wherein the Beer-Lambert law is obeyed. The temperature range for DSC and FTIR measurement was from 25 ^{o}C to 190 ^{o}C and from 25 ^{o}C to 180 ^{o}C, respectively, while for thermal expansion (TE), the temperature range was from 40 ^{o}C to 100 ^{o}C. The heating rate was 10 ^{o}C/min. for the DSC and TE measurements.

2.2. Results of the Dielectric and Elastic Study

For a polymeric material, it is well known that most of the material properties such as the dielectric constant and elastic compliance are very dispersive even at low frequencies, reflecting relatively high activation energies for the motions of molecule units and chain segments.[9] Further more, the variation in the local environment and the length of the chain segments involved in the motion results in a broad distribution of the activation energy (broad relaxation time distribution). In dealing with the electromechanical response of a polymeric material, it is advantageous to divide the segment motions into those related to the dielectric response and those related to the mechanical response, and the overlap between the two, i.e., those related to both, yields the electromechanical response of the material. In addition, it is also conceivable that the activation energies for the motions of molecular units and segments which involve the strain and stress (mechanical) might be different from that for the motions of the segments which involves little or no strain and stress. As will be discussed later in the paper, such a difference in the

activation energies between the two types of the motions will have a direct effect on the electrostrictive response of a polymeric material. Therefore, dispersion characteristics of the dielectric and elastic responses of the sample are analyzed in detail in the following.

The dielectric constant as a function of temperature is presented in figure 3. A strong frequency dispersion was observed. In the temperature range investigated, there are three relaxation peaks. The one at temperature near 20 °C is related to the glass transition which is due to the freezing process of the soft segments from a rubbery state into a glass state (α-relaxation). The one at temperatures near -100 °C is the β-relaxation which was suggested from the early studies on polyurethanes and polyamids to be related to the absorbed water molecules.[9] The nature of the relaxation at temperatures near 70 °C is unknown before and is labeled as I-relaxation here. The results of the FTIR study here suggests that it might be associated with the motion in the chain extenders.

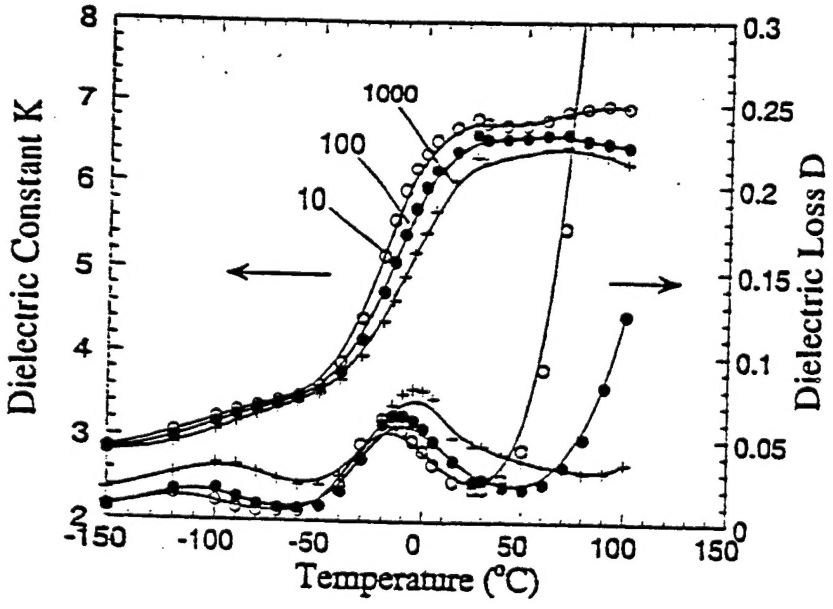

FIG. 3. Dielectric constant and dielectric loss as a function of temperature for the polyurethane elastomer where the measuring frequencies are 10 (open circles), 100 (solid circles), 1000 (plus signs) Hz.

The dielectric dispersion behavior was characterized over the frequency range from 0.01 Hz to 1 MHz and typical results are presented in figure 4(a). It was found that for the data at temperature range from -80 °C to 20 °C, one can make use of the temperature-frequency superposition principal to construct a master curve as illustrated in figure 4(b) for the one at 0 °C where the data at temperatures other than 0 °C were shifted in the frequency by times a factor a(t) (a(t) x f, where f is the frequency), which is a function of temperature t.[9] For a dielectric relaxation with a broad relaxation time distribution, the Cole-Cole single relaxation time formula should be modified. In figure 4(b), the solid line is the fitting of the data with a modified Cole-Cole equation,

$$\varepsilon^*(\omega) = \varepsilon_u + \frac{\varepsilon_R - \varepsilon_u}{1 + (i\,\omega\,\tau_0)^\beta} \qquad (1)$$

which describes the dielectric dispersion with a broad distribution of the relaxation time centered at τ_0 where ω is the angular frequency. In eq. (1), $0 < \beta \leq 1$ measures the width of the relaxation time distribution and when $\beta = 1$, eq. (1) is reduced to the single relaxation time Cole-Cole equation and a smaller β corresponds to a broader distribution of the relaxation time. For the data in figure 4(b), the fitting yields $\beta = 0.22$ indicating the existence of a broad distribution of the relaxation in the material and the τ_0 at 0 °C is 2.2×10^{-4} seconds.

In addition, it was found that the shifting factor a(t) follows the WLF relation[9]

$$a(t) = -\frac{c_1(t - t_g)}{c_2 + t - t_g} \qquad (2)$$

with $c_1 = 21.1$, $c_2 = 54.1$, $t_g = 220.0$ K. The glass transition temperature t_g at 220 K (= - 53.15 °C) is consistent with the data presented in figure 3. It should be pointed out that the parameters c_1 and c_2 obtained here are close to the universal constants c_1^g and c_2^g which have approximate

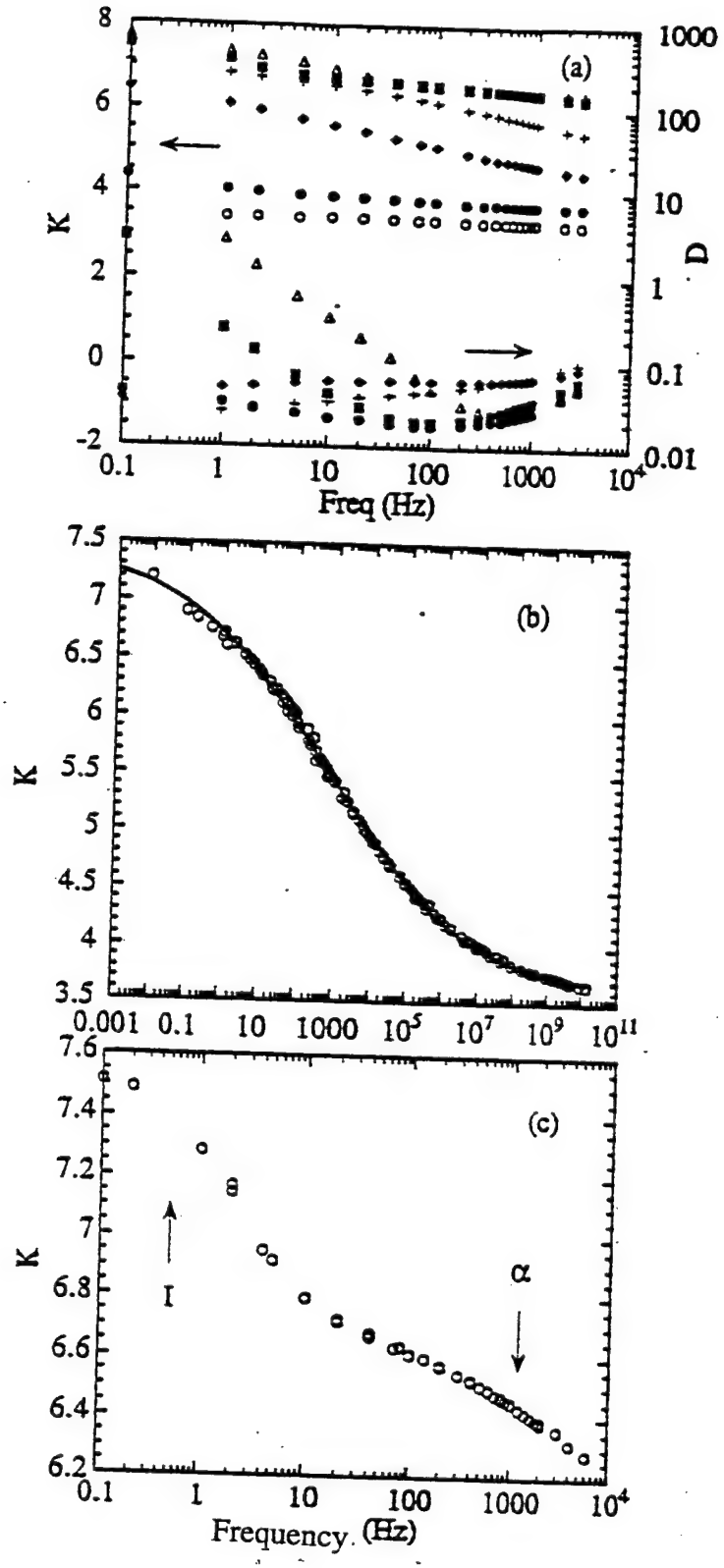

FIG. 4. (a) Dielectric constant (K) and dielectric loss (D) as a function of frequency at temperatures (from top to bottom): 80 °C (open triangles), 50 °C (solid squares), 5 °C (plus signs), −15 °C (solid diamonds), −40 °C (solid circles), and −80 °C (open circles). (b) Master curve of the dielectric constant at 0 °C where open circles are the data points and solid line is the fitting using Eq. (5). (c) Dielectric constant as a function of frequency at 60 °C which shows clearly two relaxation processes (labeled as I and α). The I-relaxation vanishes at temperatures below about 40 °C.

values of 17.44 and 51.6 respectively.[9] At temperatures above 40 °C, there is a relaxation peak (I-relaxation) in addition to the α-relaxation as shown in figure 4(c). The temperature shifting factors for the two relaxations are different as they should be. Due to this fact, no attempt was made to generate a master dispersion curve in that temperature range.

The elastic compliance measured at temperatures about the glass transition is presented in figure 5. Apparently, there is more than one order of magnitude change in the elastic compliance of the material as it goes through the glass transition. Using the temperature-frequency superposition principle, the elastic compliance curve at 0 °C over a frequency range from about 10^{-2} Hz to above 10^{3} Hz can be obtained as shown in figure 6(a). The elastic compliance

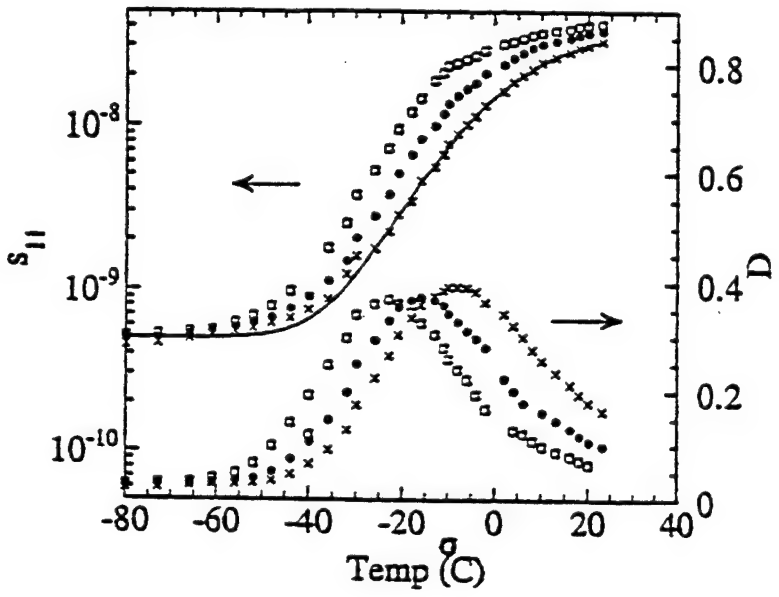

FIG. 5. The elastic compliance s_{11} and elastic loss D as a function of temperature. The measuring frequencies are 0.3 Hz (open squares), 3 Hz (solid circles), and 30 Hz (crosses). The solid line at 30 Hz data is the fitting result.

changes by more than one order of magnitude in this frequency range. The shifting factor for the elastic compliance also fits well with the WLF relation as shown in figure 6(b) yielding c_1 =

19.9, c_2 = 125.4, and a glass transition temperature t_g = 252.3 K (= -20.8 °C). The higher glass transition temperature obtained from the elastic compliance data compared with that from the dielectric constant indicates that in the polyurethane elastomer investigated, for the α-relaxation (the glass transition), the activation energy for the chain segment motions related to the strain and stress is higher than that for the motions not strain and stress related (pure dielectric). We will come back to this point later in the paper.

The data in figure 6(a) was also fitted with the relaxation equation (1) where the dielectric constant is replaced by the elastic compliance. The solid curve in figure 6(a) is the result of the fitting and apparently, the data can be described quite well by eq. (1) which yields β = 0.32 and $\tau_0 = 6 \times 10^{-2}$ seconds. Compared with the parameters from figure 4(b) of the dielectric data (at the same temperature), the average relaxation time τ_0 is longer, which is consistent with the results presented in the preceding paragraph that the activation energies for the segment motions generating strain are higher than those of non-strain related segment motions. From the fact that both eq. (1) and WLF relation describe the mechanical relaxation data rather well, we tried to combine eq. (1) with the WLF relation

$$\log \tau_0 = \log \tau_g - \frac{c_1(t - t_g)}{c_2 + t - t_g}$$

to fit the data in figure 5. Indeed, the data in figure 5 can be described well as demonstrated by the solid curve in the figure for the data at 30 Hz. The fitting yields β = 0.34, c_1 = 16.5, c_2 = 144, and a glass transition temperature t_g = 255 K. It is quite evident that the results of the fitting to the two sets of data are quite consistent with each other, especially the value of the glass transition temperature.

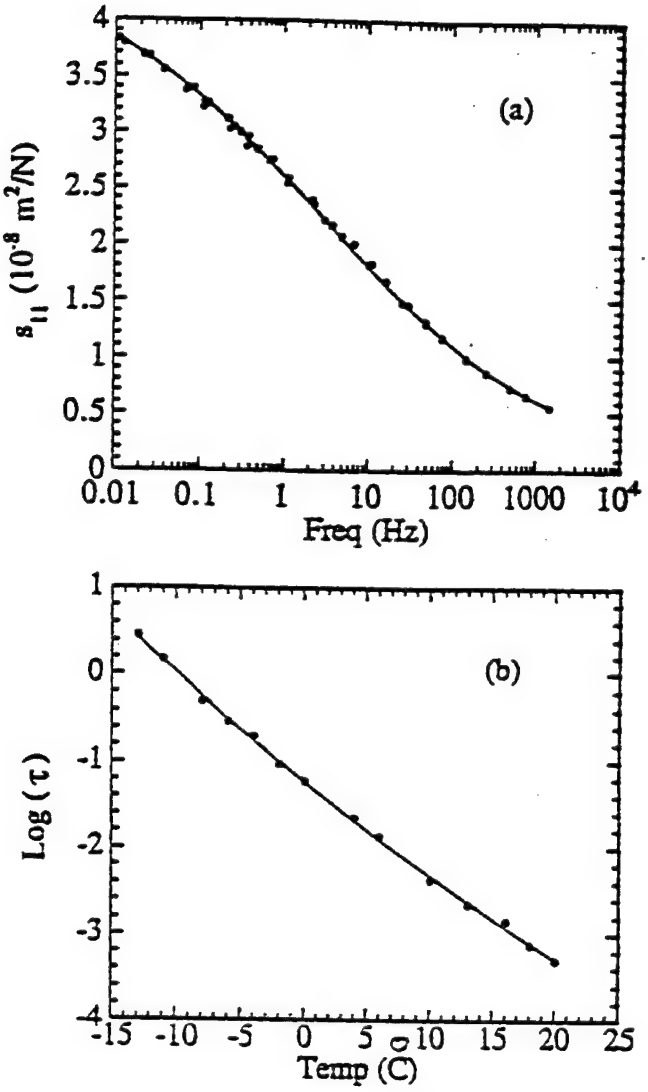

FIG. 6. (a) The master curve for the elastic compliance at 0 °C where the solid line is from the fitting and solid circles are the experimental data. (b) The change of the relaxation time τ with temperature, where τ is obtained from the elastic compliance data. Solid circles are the data points and solid line is the fitting using WLF relation.

2.3. Electrostriction and Maxwell Contribution to the Strain Response in the Materials

In general, in a non-piezoelectric material such as the polyurethane elastomers investigated, the electric field induced strain can be caused by the electrostrictive and also by the Maxwell

stress effects.[13,14] The electrostrictive effect is the direct coupling between the polarization and mechanical response in the material. It is the strain (S) or stress (T) change induced by a change in the polarization level (P) in the material which can be expressed as:

$$S = Q P^2 \qquad (3)$$

where Q is the electrostrictive coefficient of the material. For a linear dielectric where $P = \varepsilon_0 (K-1) E$, eq. (3) can be written as

$$S = Q \varepsilon_0^2 (K-1)^2 E^2 \qquad (4).$$

K is the dielectric constant of the material and ε_0 is the vacuum dielectric permittivity. On the other hand, Maxwell stress, which is due to the interaction between the free charges on the electrodes (Coulomb interaction) and to electrostatic forces that arise from dielectric inhomogeneities, can also contribute to the electric field induced strain response. For the situation considered here, it is also proportional to the square of the applied electric field (E) and it can be shown

$$T = - \varepsilon_0 K E^2 / 2 \qquad (5)$$

Hence, the dimensional change due to the Maxwell stress is

$$S = - s \varepsilon_0 K E^2 / 2 \qquad (6)$$

where s is the compliance of the material. As can be seen, for a soft material, the strain induced by the Maxwell stress can be quite substantial. In order to identify the contributions from the different mechanisms, it is necessary to measure the dielectric permittivity, the elastic compliance, and the electric field induced strain simultaneously.

It has been shown that the electric field induced strain in the polyurethane samples is proportional to the square of the applied electric field. Hence, a parameter R_{33} is introduced to describe the sensitivity of the strain response of the material to an applied electric field

$$S_3 = R_{33} E^2.$$

Presented in figure 7 is R_{33} as a function of frequency characterized in the temperature range from - 30 °C to 80 °C. R_{33} is always less than zero indicating that an applied electric field causes a contraction in the specimen in the direction parallel to the applied field. In analogy to the dielectric constant and elastic compliance, R_{33} also exhibits a strong frequency dependence.

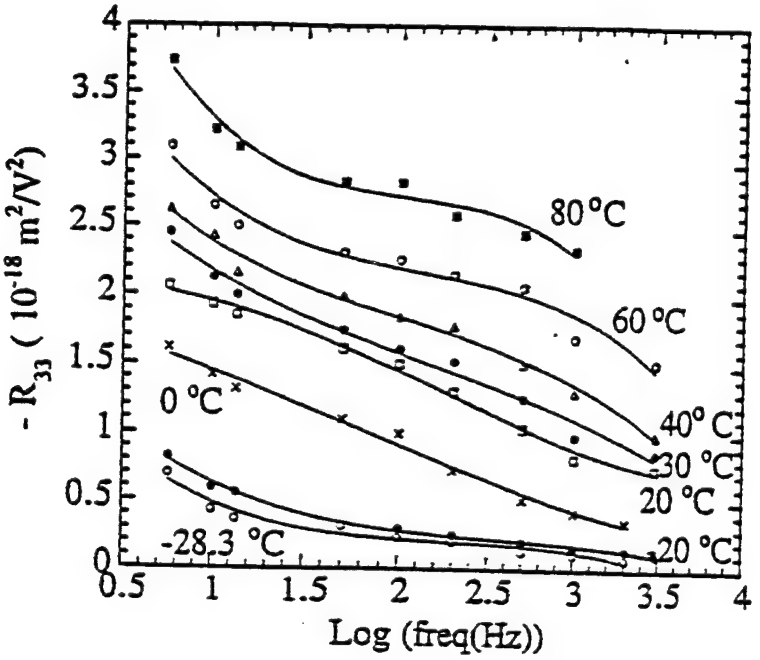

FIG. 7. R_{33} as a function of frequency at different temperatures (from top to bottom): 80 °C solid squares), 60 °C (open circles), 40 °C (open triangles), 30 °C (solid circles), 20 °C (open squares), 0 °C (crosses), −20 °C (solid circles), and −28.3 °C (open circles). The solid lines are drawn to guide eyes.

Making use of the dielectric constant and the elastic compliance data, the contribution of Maxwell stress to the total strain response in the material can be evaluated, which is shown in figure 8(a) along with the total strain response at 10 Hz and 100 Hz where the Maxwell stress term is $R_m = -s_{33} \varepsilon_0 K / 2$ and in figure 8(b), the percentage of the non-Maxwell contribution at 10 Hz and 100 Hz is presented. Evidently, at temperatures above 20 °C, the contribution from Maxwell stress

is significant. The non-Maxwell stress part or the contribution related to the true electrostriction,which is the difference in figure 8(a) between R_{33} and R_m, is also quite sizable.

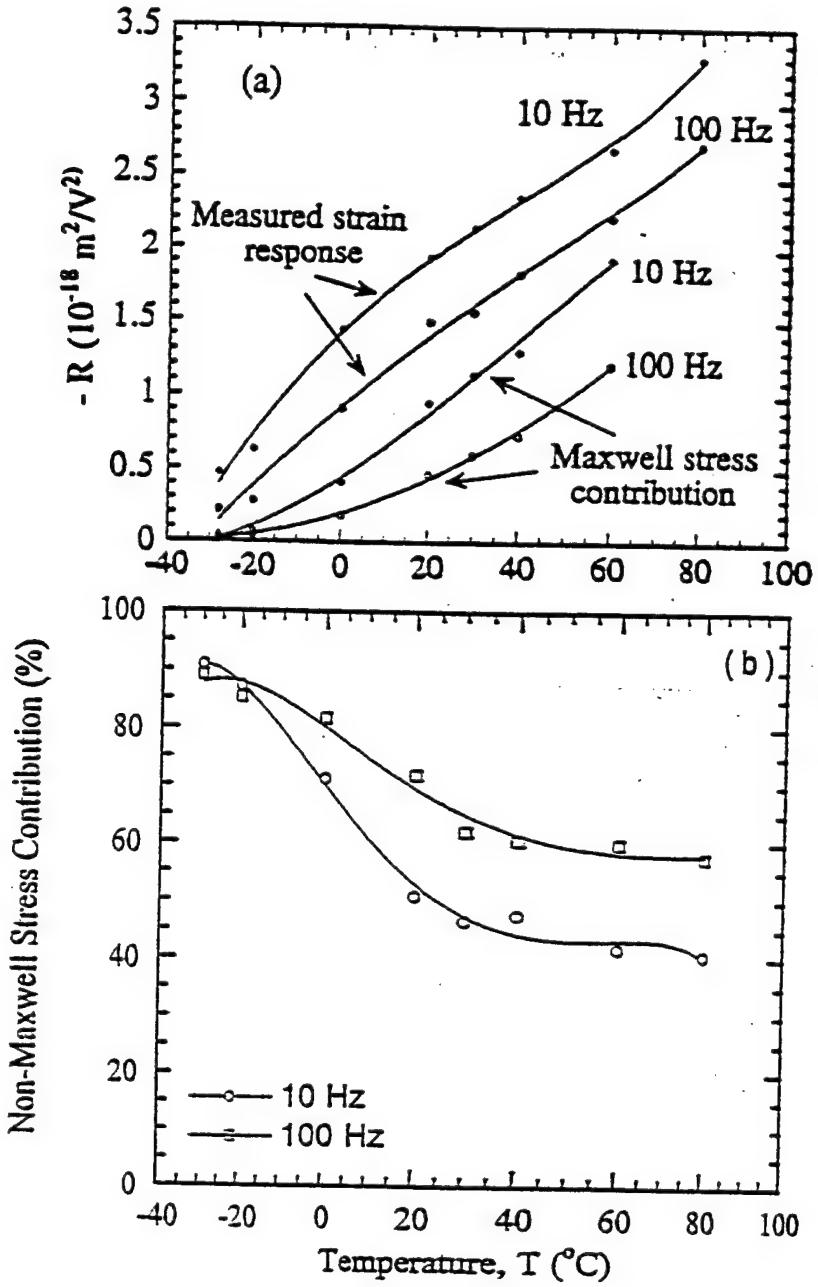

Figure 8. (a) Comparison between the measured R_{33} and the contribution from the Maxwell stress effect R_m at 10 Hz and 100 Hz. (b) The percentage of the electrostriction contribution to the total strain response at 10 Hz and 100 Hz at different temperatures. The solid lines are drawn to guide eyes.

Based on eq. (4), the electrostrictive coefficient for the material as a function of frequency and temperature is evaluated and presented in figures 9(a) and 9(b). Unlike the ferroelectric ceramic

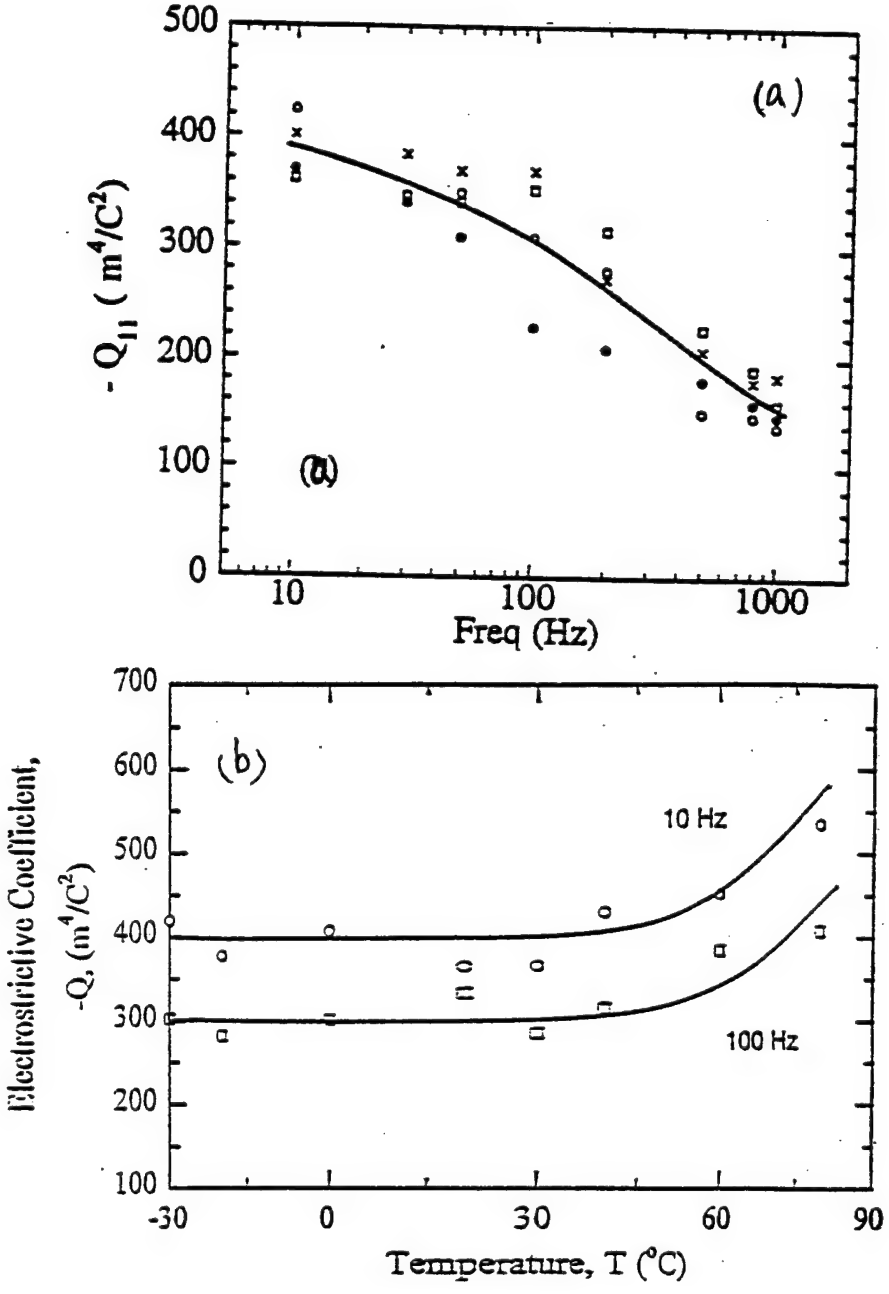

Figure 9. (a) The electrostrictive coefficient Q_{11} as a function of frequency at temperatures of -30 °C (open circles), -20 °C (solid circles), 0 °C (crosses), and 20 °C (open squares). The solid line is drawn to guide eyes. (c) The electrostrictive coefficient Q_{11} as a function of temperature in the temperature range from -30 °C to 80 °C: 10 Hz (open circles), 100 Hz (open squares). The solid lines are drawn to guide eyes.

materials where Q is nearly independent of temperature and frequency, the electrostrictive coefficient for the polyurethane elastomer depends on frequency markedly and weakly on temperature in the temperature range investigated. The relatively large data scatter in figures 9(a) and 9(b) is caused by the fact that the data are obtained from three sets of data, i.e., R_{33}, K, and s_{33}, each of which contains data scatter. The decrease of the Q with frequency indicates that the component of the polarization motions of high frequency (short relaxation times) does not generate strain in the material and hence is pure dielectric.

In Table I, the electrostrictive coefficients Q_{11} from several commonly used ferroelectric materials are compared with that of polyurethane elastomer investigated. The Q for the polyurethane elastomer investigated is much larger than those of the other materials. Although the detailed mechanisms of the electrostriction in a material depends on the molecular bases generating it such as the ionic displacement and polarization orientation effect on which very little

Table I. Comparison of the electrostriction coefficients and related properties

Materials	Q_{11} (m^4/C^2)	K	s (10^{-11} m^2/N)
PMN-PT[15,16]	0.02	25,000	1.0
PZT[17]	0.096	2,000	1.6
PVDF[6,18]	- 2.0	9	30
Polyurethane	- 150 -- 450	4 -- 8	5×10^2 -- 5×10^3

a. Q_{11} is the longitudinal electrostrictive coefficient, K is the dielectric constant, and s is the elastic compliance.

understanding exists, there exist empirical relationships which seem to be consistent with the experimental results on the electrostrictions from different materials. For instance, it has been observed that the electrostrictive coefficient Q is inversely proportional to the dielectric constant and proportional to the elastic compliance of the material.[14] As shown in Table I, these rules can qualitatively describe the data for PMN, PZT and PVDF. However, for the polyurethane elastomer, in the temperature range from -30 C to 20 C, the elastic compliance reduces more than one order of magnitude (figure 5) while the change of Q in the same temperature range (figure 9(b)) is relatively minor, which seems not consistent with the empirical rule between Q and compliance of the material. On the other hand, in the temperature range corresponding to second transition (I-relaxation), the electrostrictive coefficient Q exhibits increase with temperature. Considering the fact that the electromechanical response of a polymer material is contributed by the molecular motions which participate in both the polarization and elastic processes, the increase in the electrostrictive coefficient Q is a result of the increased elasticity per unit polarization change, which can be caused by lowering the energy barrier for the mechanically related segment motion as reflected by the increase in the elastic compliance in this temperature range, where the dielectric constant does not show much change.

The difference in the glass transition temperatures observed from the dielectric data and the elastic compliance data indicates that in the polyurethane elastomer investigated, the chain segment motions can be divided into those generating the mechanical response and those generating the dielectric and polarization response. The overlap between the two, i.e., those generating both the mechanical and polarization, yields the electromechanical response in the material. In addition, the dispersion of the electrostrictive coefficient Q, i.e., the observed decrease of Q with frequency, indicates that the high frequency components of the polarization motions do not contribute to the strain response as much as the low frequency components which implies that the activation energies for the polarization motions generating strain response are higher than those for non-strain related polarization changes. These are consistent with the facts

that the glass transition temperature T_g from the elastic compliance data is higher than that from the dielectric data and the there is a large drop of the electric field induced strain response at temperatures near T_g of the elastic compliance data.

2.4 DSC, FTIR, and Thermal Expansion Measurements

To understand how the observed macroscopic properties are related to the molecular structures, molecular motions and transitional phenomena, Differential Scanning Calorimetry (DSC), Fourier Transform Infrared (FTIR) spectroscopy and Thermal Expansion (TE) measurements of the polyurethane were examined as functions of temperature.

As has been shown in figure 8(a), the strain coefficient, R_{33} increases with temperature and decreases with frequency. In the temperature range from -30 ^{o}C to 60 ^{o}C, two relatively sharp increments are observed: one starts at the temperature about -20 ^{o}C and the other starts at about 50 ^{o}C. Similar trends are also observed in the dielectric and elastic data shown in figures 3 and 10, respectively. The dielectric constant, K, shows a rapid increase at about -20 ^{o}C but a relatively small change at about 60 ^{o}C while the temperature dependence of the elastic compliance shows two rapid increases starting at about -25 ^{o}C and 60 ^{o}C, respectively. The sharp change in the material properties at the lower temperature, observed in these measurements, is related to the glass transition of the polyurethane due to large scale molecular motions of the soft segments, PTMEG.[19] In order to understand the change at higher temperature transition, DSC, FTIR and TE investigations, which are employed extensively in studies of structures and molecular motions of segmented polyurethane elastomers,[19-21] were carried out. The DSC curve, shown in figure 11, exhibits an endothermic peak at about 75 ^{o}C, starting at about 50 ^{o}C and ending at about 90 ^{o}C, which is much higher than the glass transition temperature, (about -20 ^{o}C) and much lower than the melting temperature, (about 170 ^{o}C), which is reflected by another endothermic peak starting

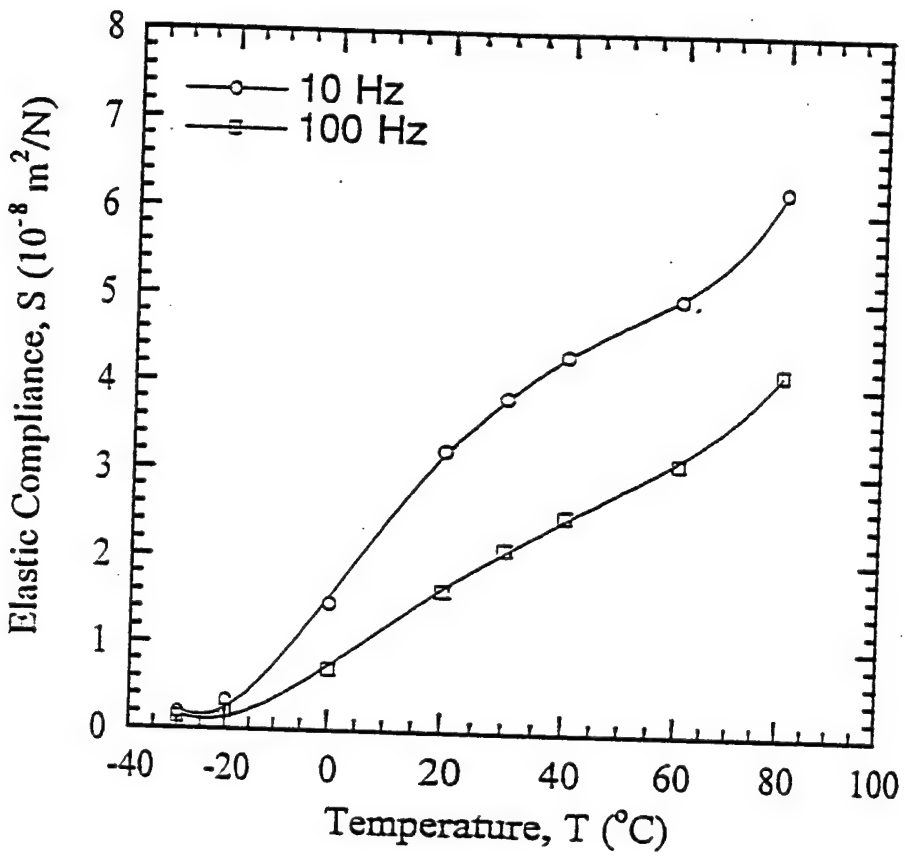

Figure 10. The elastic compliance, s, of the polyurethane elastomer (Dow 2105-80AE), at 10 Hz and 100 Hz. The solid line are drawn to guide the eye.

at about 100 °C and ending at about 185 °C. From the DSC results, the enthalpy change associated with the transition between 50 °C and 100 °C was calculated by assuming the change is associated with the dissociation of the hydrogen bonding in hard segments since some previous publication suggested the endothermic peak might be associated with hydrogen bonding dissociation. However, the value obtained, which is 3.71 kcal/mol., is obviously lower than the previously reported enthalpy change due to hydrogen-bond dissociation in segmented polyurethanes having similar chemical structure.[22] The thermal expansion

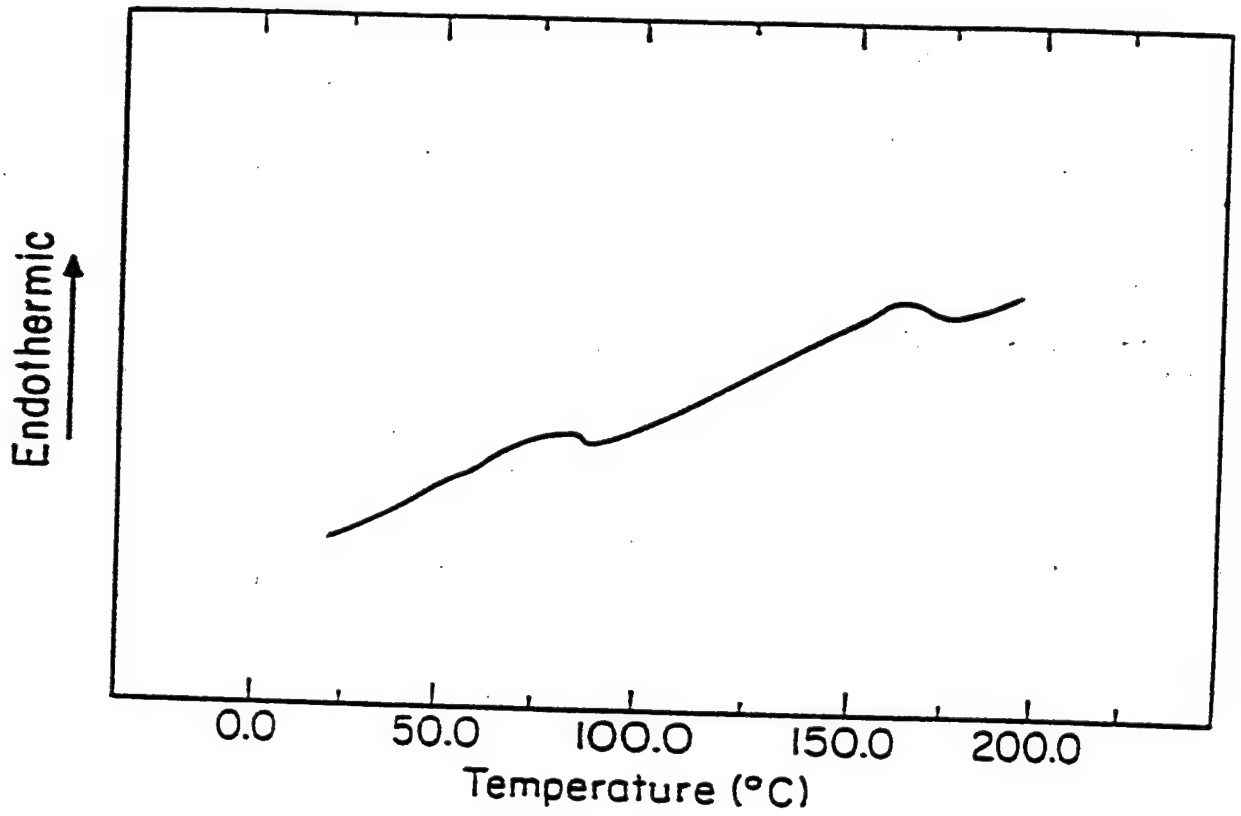

Figure 11. Differential Scanning Calorimetry (DSC) trace of the segmented polyurethane (Dow 2105-80AE) elastomer, from 25 °C to 190 °C.

measurement of the segmented polyurethane elastomer also exhibits a characteristic transitional change in the temperature range between 50 °C and 100 °C. As can be seen in figure 12, the material exhibits a rapid thermal expansion in the temperature range from about 50 °C to about 90 °C.

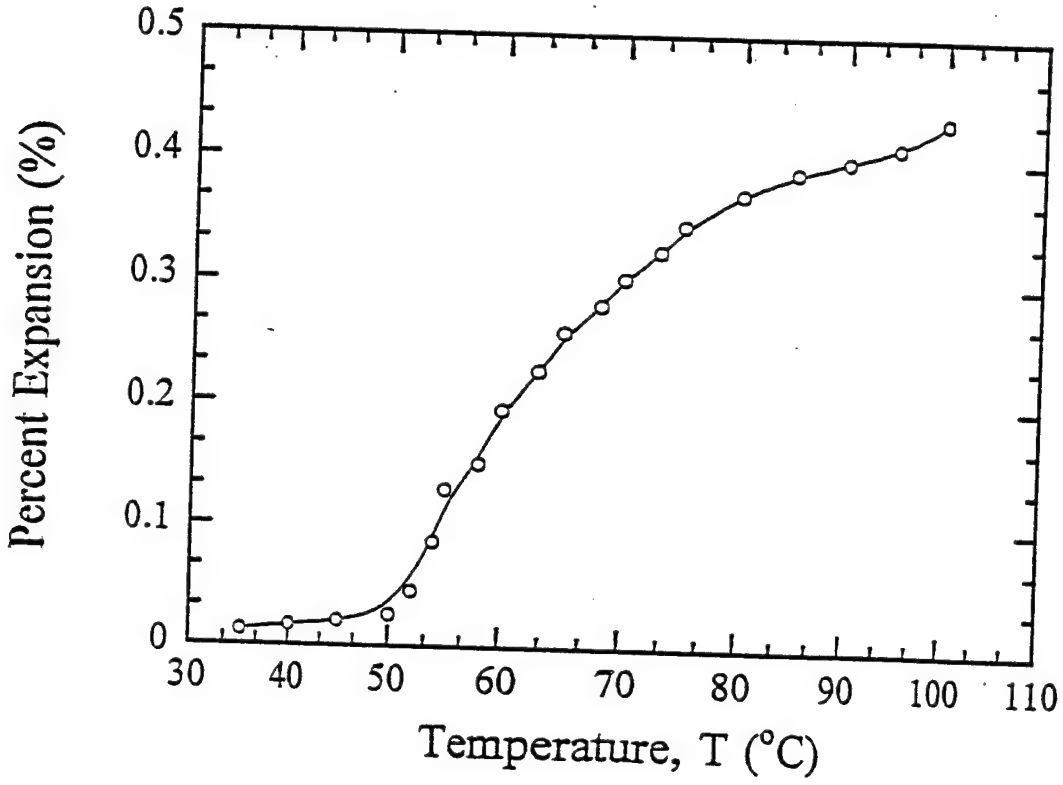

Figure 12. The thermal expansion measurement of the segmented polyurethane elastomer exhibits a transitional characteristic change in the temperature region from 50 °C to 100 °C.

The temperature dependence of the absorbency spectroscopy of the FTIR study on the polyurethane is shown in figures 13(a)-13(d). The change in the infrared absorption related to the -NH and -C=O related hydrogen bonding was investigated at 60 °C, 100 °C, 140 °C and 180 °C. As the temperature is increased from 60 °C to 100 °C, the absorption of bonded -NH (3327 cm^{-1}) associated with the absorption of bonded -C=O (1714 cm^{-1}) show only a minor decrease. The absorption of unbounded, or free, -NH (3448 cm^{-1}) and the unbonded -C=O (1730 cm^{-1}) shows very little increase in the same temperature range, which indicates that the transitional change observed in the DSC and TE measurements is not mainly

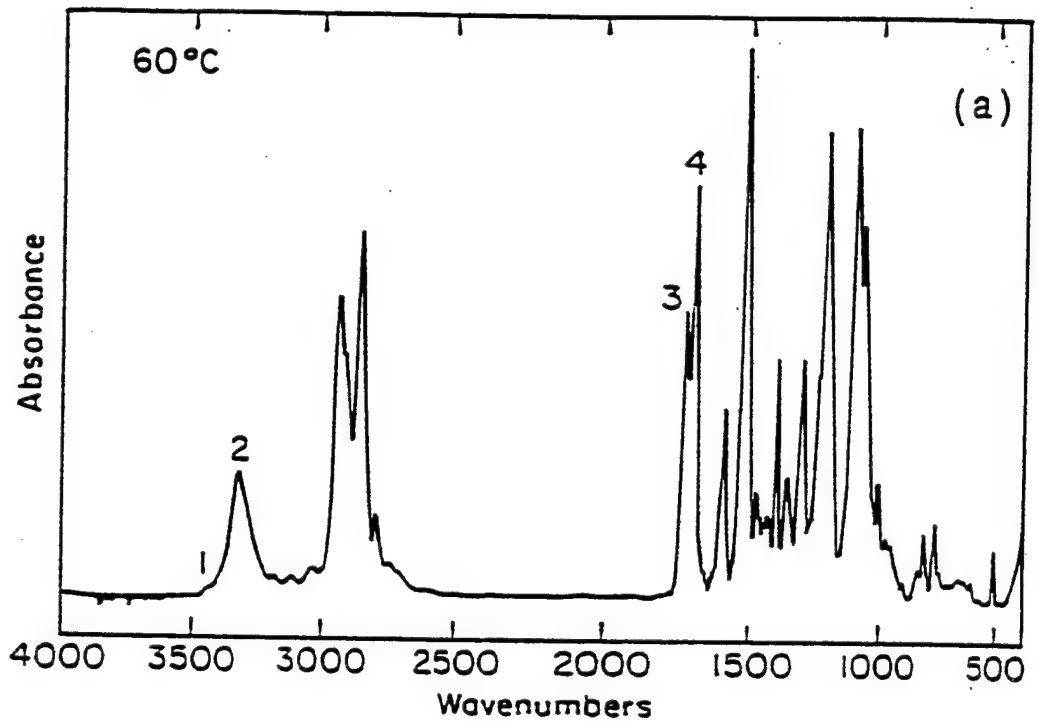
60°C
(a)
Absorbance
1
2
3
4
4000 3500 3000 2500 2000 1500 1000 500
Wavenumbers

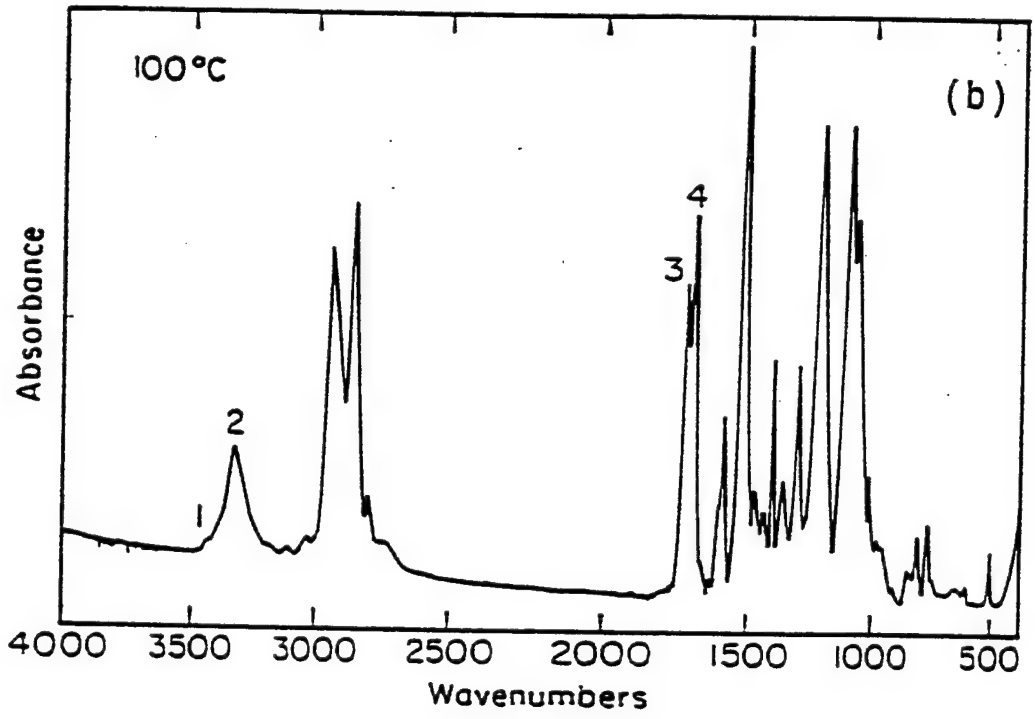
100°C
(b)
Absorbance
1
2
3
4
4000 3500 3000 2500 2000 1500 1000 500
Wavenumbers

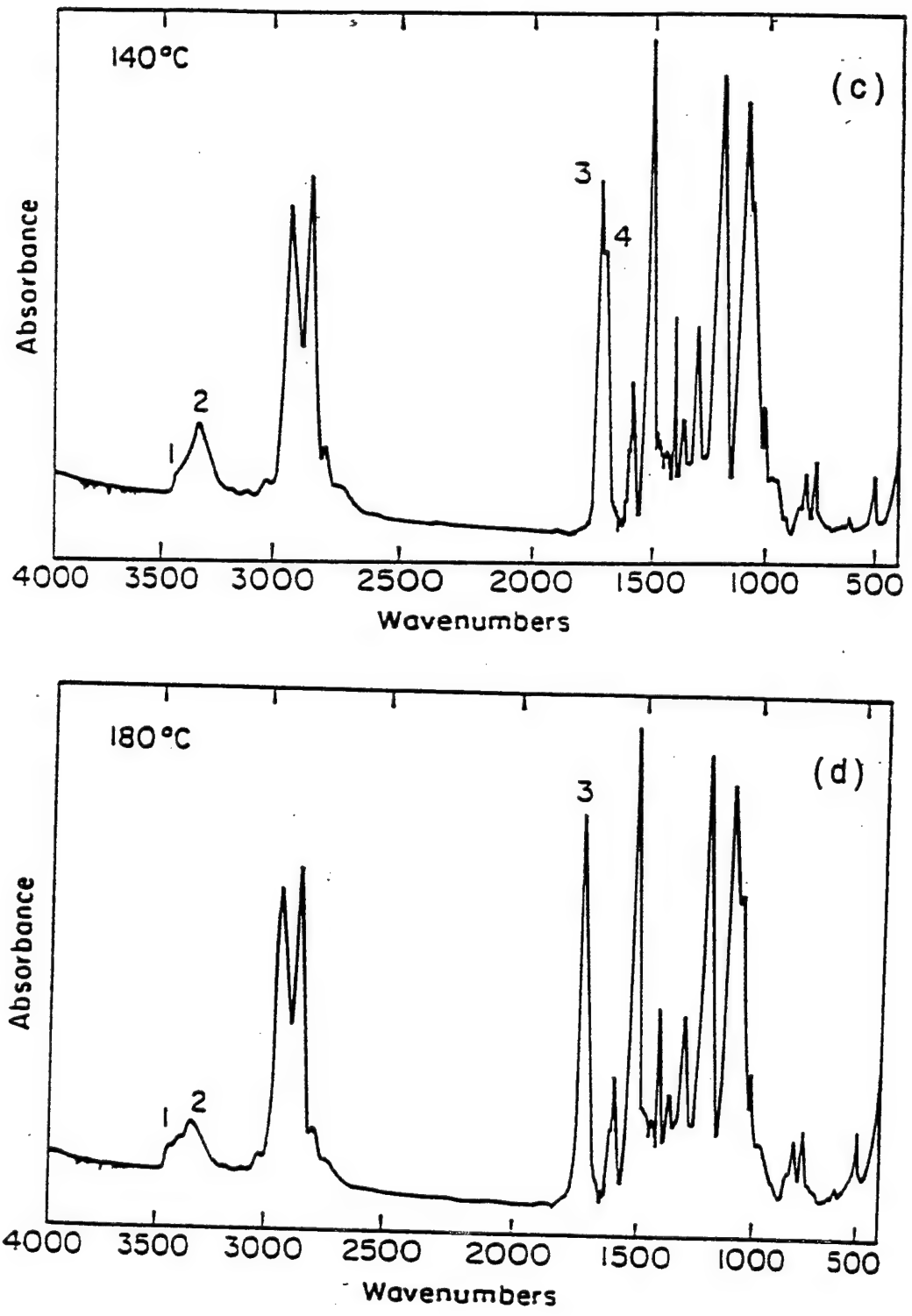

Figure 13. FTIR spectroscopy of the polyurethane elastomer (Dow 2105-80AE) at (a) 60 °C, (b) 100 °C, (c) 140 °C and (d) 180 °C. (Absorbency wavenumber: 1: 3448 cm^{-1}, 2: 3327 cm^{-1}, 3: 1730 cm^{-1}, and 4: 1714 cm^{-1}).

associated with the dissociation of the hydrogen bonding in the MDI segments. However, when the temperature is increased from 100 ^{o}C to 140 ^{o}C, a relatively large change, i.e. a large drop, in the absorption of the H-bonded groups and increase in the absorption of the unbonded groups, can be observed. Further increase of the temperature to 180 ^{o}C results in a significant dissociation of the hydrogen bonding, which is reflected by the disappearance of the bonded -NH (3327 cm^{-1}) and -C=O (1714 cm^{-1}) absorption peaks, and the large increase of the absorption peak due to the unbonded -NH (3448 cm^{-1}) and -C=O (1730 cm^{-1}). This observation corresponds to the endothermic peak observed in the temperature region from 100 ^{o}C to 180 ^{o}C in the DSC measurement, which is associated with the hard segment dissolution (melting) as a consequence of the dissociation of the hydrogen bonding in MDI segments.

The experimental results obtained from the DSC, TE and FTIR investigations show that the transition between 50 ^{o}C and 100 ^{o}C, which might be the key factor resulting in the increased field induced strain response of the segmented polyurethane in the temperature region, is neither the glass transition nor the melting if the glass transition reflects the molecular motion of the soft segments and the melting reflects the molecular flow of whole polymer chains when the hydrogen bond dissociation occurs. The molecular origin of the transition might be related to the molecular motion of the extenders within the hard segments, which might occur without destroying the hydrogen bonding sheet structure,[20] and result in expanding in the direction perpendicular to the hydrogen bonding sheets and increasing free volume. When this happens, it should lead to transitional changes in elastic and thermal expansion properties, as observed in figures 10 and 12, respectively. The asymmetric endothermic peak, i.e. slow increase before the peak position (about 75 ^{o}C) and rapid decrease after the peak observed in the DSC curve, could be a result of the restraining of the hydrogen bonding in MDI segments to the extender (Bdiol) related molecular motion. This restraint can limit the molecular motion of extenders between MDI segments, which results in the slow increase. When temperature is high enough to cause

the motion of or dissociation of the hydrogen bonds in the hard segments to a significant level, the limited molecular motion of the extenders can be accelerated, which results in the rapid decrease.

III. Development of a Novel Bimorph Based Dilatometer for Electric Field Induced Strain Characterization in Soft and Thin Polymer Films

3.1. Introduction.

Polymeric materials have many attractive and unique features for electronic and electromechanical transduction applications. In these applications, how the material behaves under an external electric field is of prime concern in the material selection. Because of the softness of samples to be characterized, currently it is still a great challenge to reliably determine the strain induced by an external electric field in thin polymer films without imposing constraint.

In general, the existing techniques for characterizing the electric field induced strain response in a polymer film can be grouped into two categories: the contact methods and non-contact methods. The contact methods such as the one making use of the change in capacitance between two parallel plates to measure the dimensional change of a polymer film are typically difficult to be used on routine bases.[7,23] In addition, the contacts from the capacitor plates in the capacitance method may impose mechanical constraints in the sample which could be significant for a soft and thin sample and introduce large error in the measurement. For the non-contact measurements, where the laser dilatometer is the one most frequently used, in order to determine the field induced strain in the out-of-plane direction in thin films, two laser beams on the opposite faces of the sample are required. However, again because of the thinness and softness of the films, it is quite easy to excite the flexure motion in the sample which causes severe errors in the results.[24] It appears to us that currently there exists no suitable technique to characterize the electric field induced strain in thin and soft polymeric samples reliably and conveniently.

The recent development of the atomic force microscope has demonstrated the high sensitivity of a cantilever beam in detecting small force, which implies that the similar principle may be transplanted to measure the displacement of soft polymer films without imposing large stress or mechanical constrains in the sample.[25,26] In an even more traditional area, i.e., displacement sensor in a phonograph cartridge, the demands of audiophiles have been forcing the constant improvement of the sensor head and as a result, phonograph cartridges are well developed high sensitivity transducers which require a very small contact force and can be operated over a wide frequency range. Inspired by these advancements, we attempted to develop a high sensitivity displacement sensor to characterize the electric field induced strain in soft and thin polymeric samples based the piezoelectric bimorph cantilever beam, which in the current device was modified from a phonograph pick-up cartridge, and the results are reported in this paper.

3.2. Experimental

The schematic of the set-up is shown in figure 14. Under an external electric field, the sample expands and contracts in the z-direction and generates a corresponding motion in the sensor head. Consequently, a bending in the piezoelectric bimorph is produced. Through the direct piezoelectric effect, an electrical output which is proportional to the sensor head displacement is generated. Through a simple calibration procedure, this output signal can be used to quantitatively measure the displacement. In the current set-up, a well aged PZT-4 piezoceramic is used as the displacement standard, whose piezoelectric d_{33} value was measured by both a laser dilatometer and a Berlincourt d_{33} meter.[12,27] By applying a fixed voltage to this standard, typically in the range between 1 to 10 volts, a displacement in the range of 2 - 20 Å is generated to calibrate the device. A typical calibration curve thus obtained is shown in figure 15 where the measured current from a lock-in amplifier vs. the displacement in the PZT-4 standard is presented against the measuring frequency. The dimensions of the PZT-4 standard is 5*5*5 mm^3. The lock-in amplifier used is Model SR830 from Stanford Research Systems which has a current sensitivity down to the fA range.

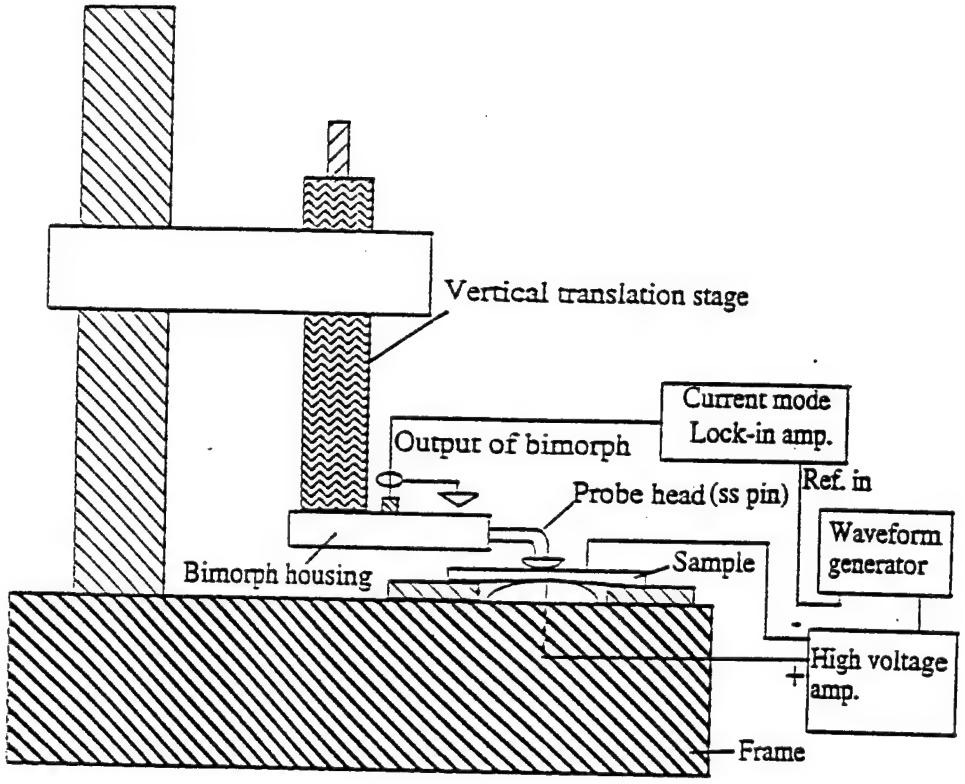

(a)

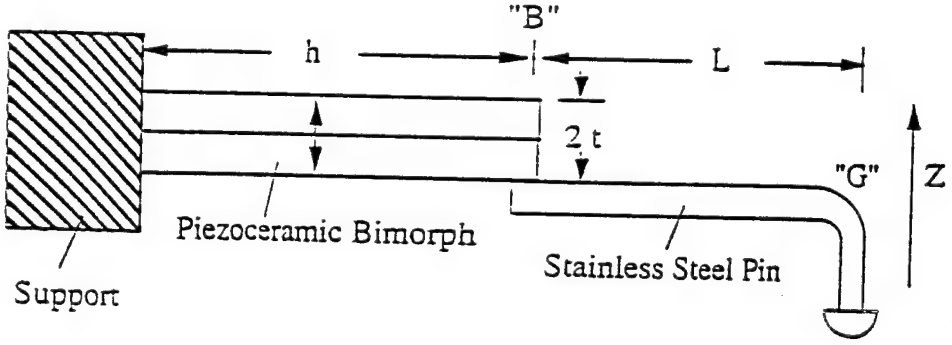

(b)

Figure 14. (a) Schematic of the newly developed high resolution displacement sensor and the electric driving and detection circuits; (b) Schematic of the sensor head consisting of a piezoceramic bimorph and a stainless steel pin. The bending in the bimorph generates an electric output which is proportional to the displacement at the point G.

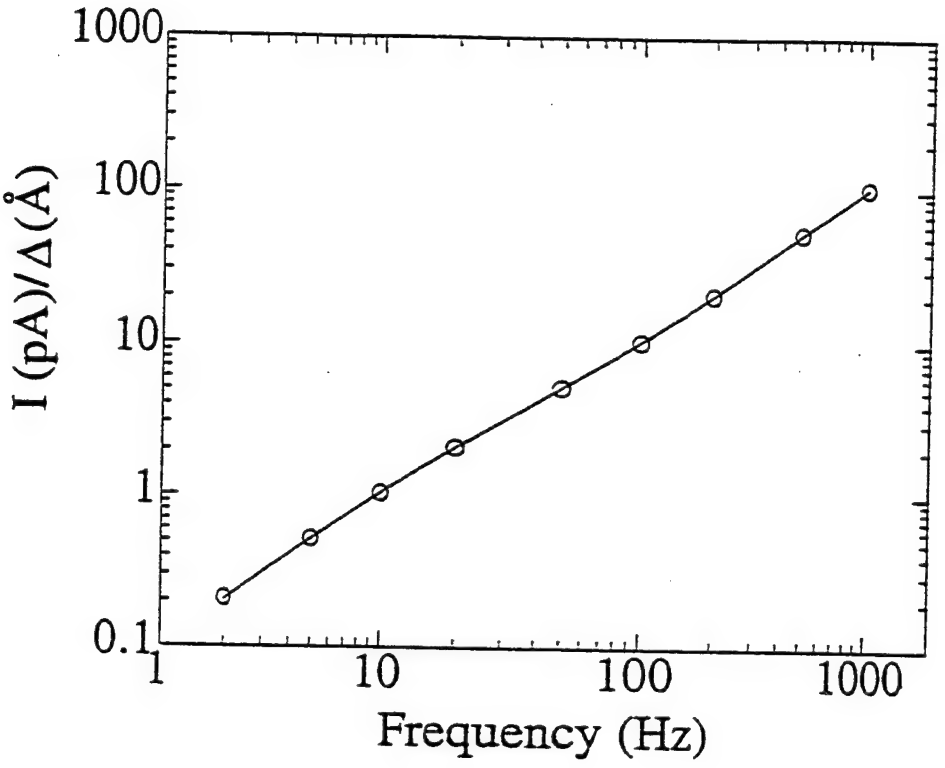

Figure 15. The calibration curve of the displacement sensor which shows that the sensitivity of the device is proportional to the frequency. Open circles are the experimental data and solid line is a linear fitting curve.

3.3. Analysis of the Performance

Using the constitutive equations for a piezoelectric ceramic material, the relations among the displacement δ^b at the point B, the force F at the tip, and the charge q and voltage output V of a bimorph supported at one end under static condition can be derived (as shown in figure 14(b)):

$$\begin{pmatrix} \delta^b \\ q \end{pmatrix} = \begin{pmatrix} \frac{s_{11}^E h^3}{2wt^3} & -\frac{3d_{31}h^2}{8t^2} \\ -\frac{3d_{31}h^2}{8t^2} & \frac{\varepsilon_{33}^T hw(1-k_{31}^2/4)}{2t} \end{pmatrix} \begin{pmatrix} F \\ V \end{pmatrix} \qquad (7)$$

where s_{11}^E is the elastic compliance of the piezoceramic, w is the width of the bimorph, d_{31} is the transverse piezoelectric coefficient, ε_{33}^T is the dielectric permittivity, and k_{31} is the electromechanical

coupling factor, respectively.[28] In our experimental situation, the short circuit condition is used which implies V = 0 in the equation (7).

For the stainless steel (ss) pin attached to the end of the bimorph, a force F at the tip G will produce a bending according to[29]

$$\delta^s = \frac{2L^3 s^{st}}{3\pi r^4} F \qquad (8)$$

where r is the radius of the ss pin which is 0.32 mm in the current device and s^{st} is the elastic compliance of the ss pin. In addition, the bending in the piezoceramic bimorph will also produce a displacement at the point G, which can be shown through the geometric consideration:

$$\delta' = \left(\frac{h^3 s_{11}^E}{2wt^3} + \frac{3h^2 L s_{11}^E}{2wt^3}\right) F \qquad (9)$$

where the first term on the right hand side of the equation is the displacement at the end of the bimorph (point B in figure 14(b)) and the second term is just a geometric amplification effect. Combining this with the bending at the stainless steel pin (eq. (8)) yields the relationship between the force F and displacement Δ at the sensor head (point G):

$$\Delta = \delta^s + \delta' = \mathrm{B}\,\mathrm{F} \qquad (10)$$

where $\mathrm{B} = \frac{2L^3 s^{st}}{3\pi r^4} + \frac{3h^2 L s_{11}^E}{2wt^3} + \frac{h^3 s_{11}^E}{2wt^3}$. Similarly, the charge output from the sensor head (piezoelectric bimorph) is given by

$$q = -\frac{3d_{31}h^2}{8t^2} F \qquad (11)$$

Since we are interested in the displacement sensing, combining eqs. (10) and (11) produces

$$q = -\frac{3d_{31}h^2}{8t^2 B} \Delta \qquad (12)$$

In our set-up, L is approximately the same as h and hence, B in eq. (12) is proportional h^3. Eq. (12) indicates that for a fixed displacement Δ at point G, a short length (smaller h and L) in the

sensor head will improve the sensitivity. The reason behind this is that for a fixed displacement Δ, a shorter length will result in a large force F in the bimorph (eq. (10)) which results in a high charge output. As a result, the sensitivity of the bimorph sensor is approximately inversely proportional to h and L. However, for the strain measurement in soft polymer films, a large force at the sensor head will inevitably introduce a large error, which certainly imposes limit on the lengths of h and L in the device.

3.4. Experimental Results

Figure 16(a) presents the relationship between the current output of the sensor head and driving electric field applied to the PZT-4 standard (the displacement is linearly proportional to the driving field). The data shown are at 100 Hz, 400 Hz, and 1 kHz. Since for a fixed displacement Δ, the charge output q is fixed and for a sinusoid signal, the current output I from the bimorph is equal to q ω, where ω is the angular frequency. The sensitivity of the system which is defined as I/Δ, hence, will be directly proportional to the frequency. On the other hand, the environmental noises such as the vibration and air turbulence, which in the current system are the major source limiting the probe sensitivity, will become severe at low frequencies. Due to this reason, the measured sensitivity (or displacement resolution) limit of the system vs. frequency, as shown in figure 16(b), falls off faster than 1/f. The data in figure 16(b) is from the error bar $\delta\Delta$ ($\Delta \pm \delta\Delta$), which is defined as the half width at half maximum of the displacement data for a given applied voltage. To reduce these noises, the set-up was placed inside a closed chamber during the measurement. The data in figure 16(b) show that the probe has a sub-Angstrom sensitivity over a relatively wide frequency range. For instance, at 100 Hz, it can detect a displacement of 0.01 Å.

The data at 100 Hz were also used to make a comparison between the test result and the performance prediction based on the static model presented in the preceding section. Since in the

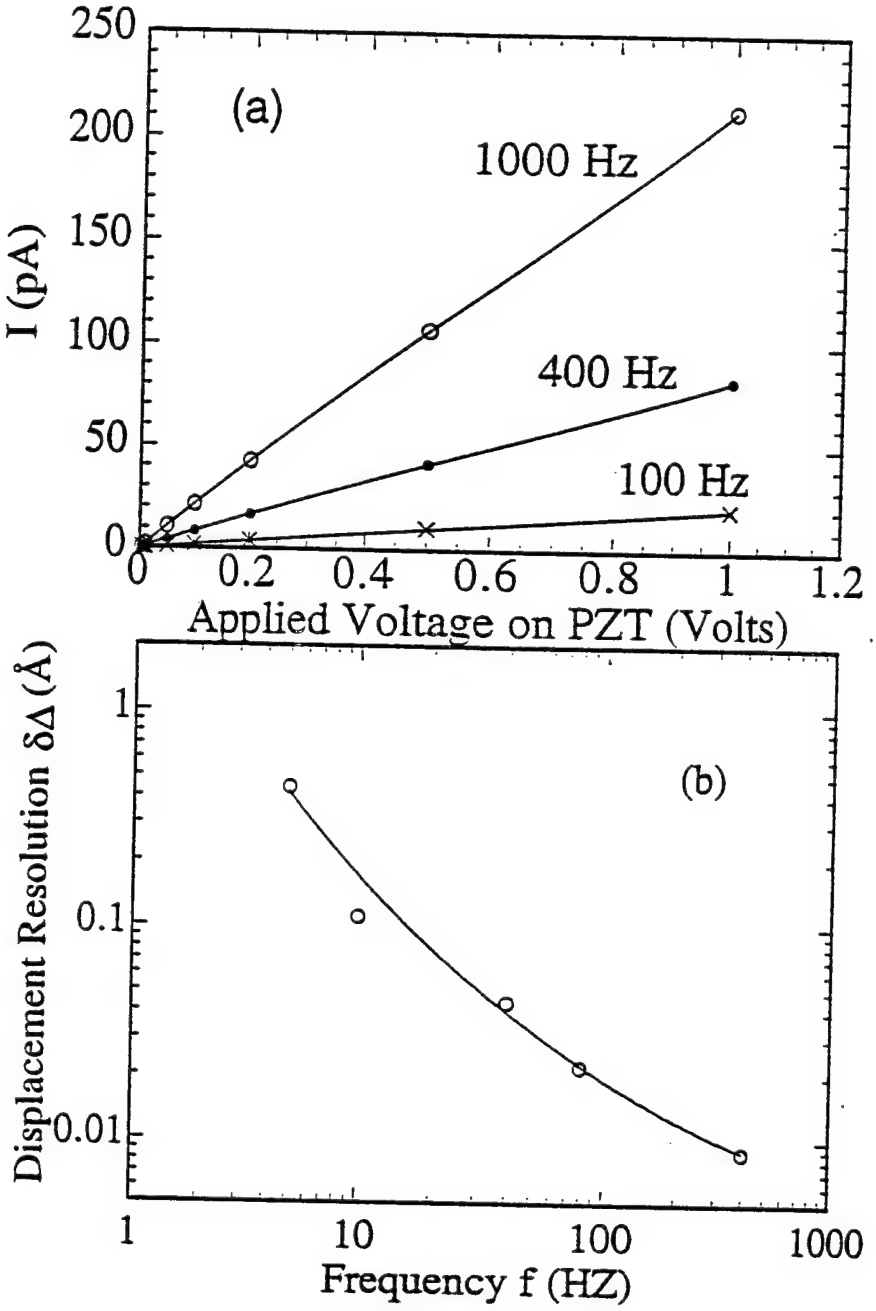

Figure 16. (a) The current measured by a Lock-in amplifier vs. the displacement in a PZT-4 standard (the displacement in PZT-4 = 2.20 Å * applied voltage) which shows a linear relationship between the displacement and the current output. The sensitivity of the device decreases at low frequency. Open circles, black dots, and crosses are the data points and solid lines are drawn to guide eyes. (b) The displacement resolution limit of the device vs. frequency. Apparently, the resolution limit drops off faster than 1/f. Open circles are the data and solid curve is drawn to guide eyes.

construction of the sensor head, the exact dimensions such as h and L cannot be controlled precisely, the approximate values of h = 10 mm, and L = 10 mm are used in the calculation. The other parameters are: for the piezoceramic bimorph, t = 0.3 mm, w = 1.5 mm, s_{11}^{E} = 16.5 *10^{-12} m^2/N, and d_{31} = -274 pC/N, and for the ss pin, r = 0.32 mm, s^{st} = 5.2 * 10^{-12} m^2/N. Using these parameters, we obtain the charge output 1.50*10^{-15} C for a displacement at the sensor head of 11.04 Å, which is very close to the experimentally measured value of 1.59*10^{-15} C (data in figure 16(a)). Such a good agreement between the model prediction and the test result could be a coincidence. However, it does indicate that the probe functions properly with a high sensitivity.

One of the concerns in operating this new instrument is its operational frequency range. At the low frequency end, the frequency limit is mainly caused by the decrease of the sensitivity as the frequency is lowered. On the other hand, on the high frequency end, it is the resonant frequency of the system which limits how high the probe can be operated. For a cantilever beam, the resonant frequency is inversely proportional to the square of the length (h and l for the system discussed here).[28,29] Shown in figure 17 is the electric impedance of the probe head (the impedance is from the

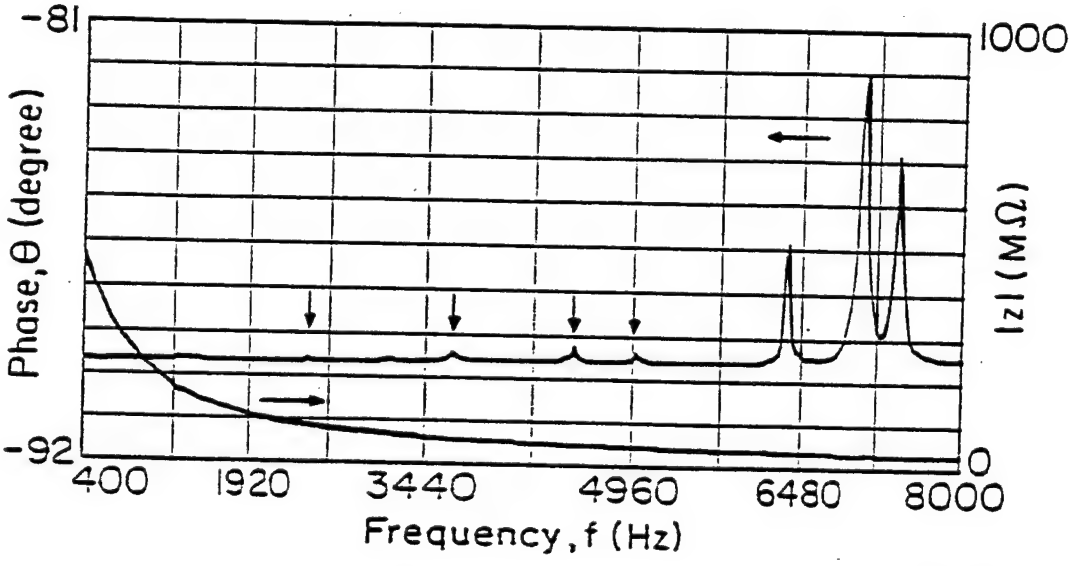

Figure 17. The electric impedance curve measured from the piezoelectric bimorph when the probe head was in contact with a sample. There is no noticeable resonance at frequencies below 2 kHz (the weak resonances are indicated by arrows). Hence, the current device can be used up to 1 kHz without the interference of the resonance. The resonant frequency in the device can be raised by reducing the lengths of the bimorph and ss pin.

piezoelectric bimorph) vs. frequency for the system tested where the probe head is in contact with a sample as in the measurement situation. As seen, the first resonance mode appears at a frequency above 2 kHz. From the fixed boundary condition at the two ends, this resonance corresponds to a half-wave length resonance. Hence, the device can be used at frequencies up to 1 kHz without the interference with the resonant mode which was also confirmed by direct experimental results.

After the calibration and evaluation of the device, a series of polyurethane elastomers (DOW 2103-80AE) was characterized as to their field induced strain responses. In the temperature range about room temperature, the compliance of the polyurethane samples is below $5*10^{-8}$ m^2/N and, the device can be used to determine the field induced strain without introducing significant error.

Since in this type of material, because of the central symmetry, the strain S is proportional to the square of the applied electric field E, i.e., $S = RE^2$, where R is a coefficient describing the sensitivity of strain change in the material to the external electric field. For a sinusoidal applied electric field $E= E_0 \cos \omega t$, it is the 2f component of the strain response that is measured by the lock-in amplifier,

$$S = R (E_0 \cos \omega t)^2$$

$$= R E_0^2 (1-\cos 2\omega t) / 2 \qquad (13)$$

and the displacement amplitude Δ measured at the probe head at 2f frequency is

$$\Delta = t_p R E_0^2 / 2$$

Shown in figure 18 is the R coefficient for polyurethane films vs. thickness at different frequencies measured at room temperature. The samples are solution cast films of DOW polyurethane 2103-80AE and the electrode is sputtered gold film of about 300 Å thickness. The negative sign of R coefficient shows that the film contracts as an electric field is applied. The device is quite convenient in measuring the electric field induced strain in thin film samples and the thinnest film measured here is 20 μm. From the basic principle of the device and the analysis presented, it is clear that the probe

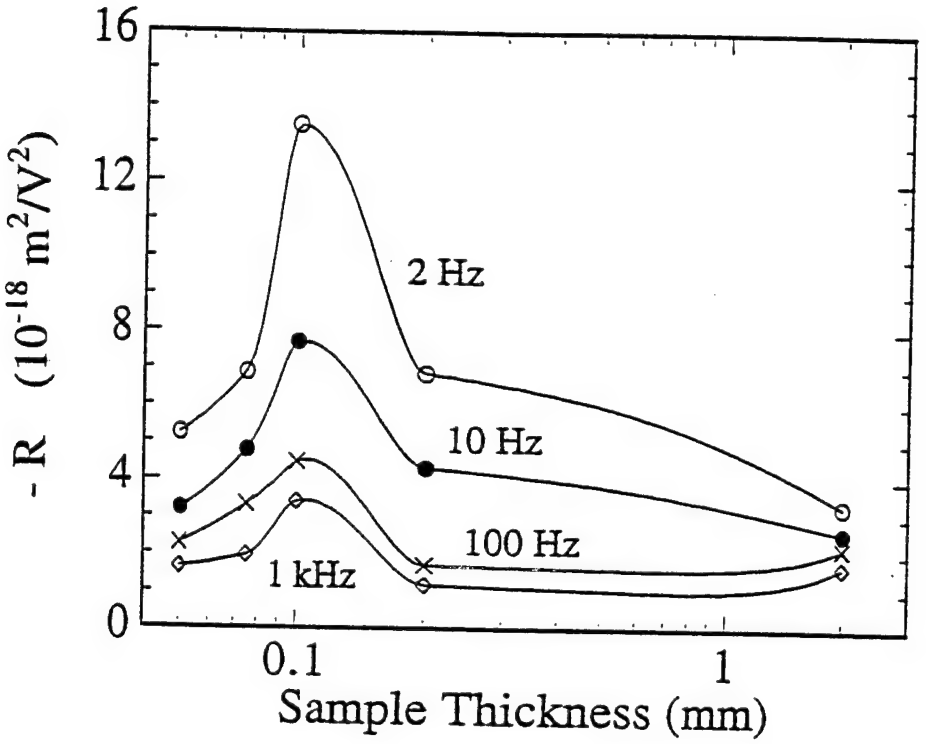

Figure 18. R of a polyurethane elastomer (DOW 2103-80AE) as a function of the sample thickness at different frequencies. The negative sign of R coefficient indicates that the film contracts when a voltage is applied. The thinnest sample measured is 20 μm thick. Data points are shown on the figure and the solid curves are drawn to guide eyes.

can be used to characterize the strain response in even thinner films. The dependence of R with thickness has been investigated earlier and due to the limitation of the measuring technique (a laser beam dilatometer), the thinnest sample examined was 0.15 mm.[6,24] In the thickness range overlapped, the results from the two measurements are consistent with each other. Figure 19 presents a comparison between the result measured from the current device and that from a double beam laser dilatometer on polyurethane sample of 2 mm thickness. Apparently, the results from the two agree with each other quite well.

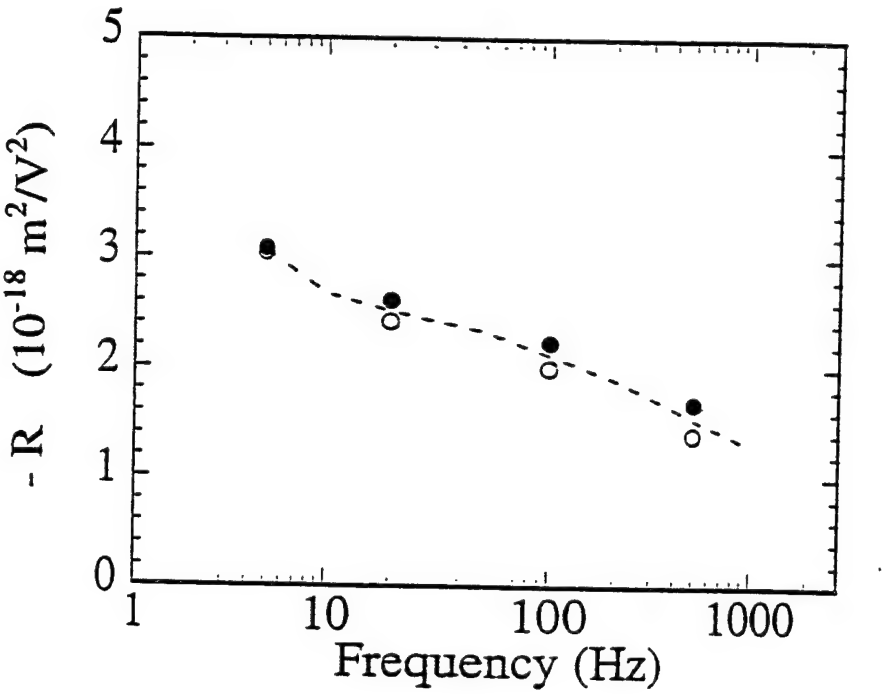

Figure 19. Comparison of R coefficient of a polyurethane sample (2 mm thick) measured from a double beam laser dilatometer (solid circles) and the newly developed bimorph dilatometer (open circles) as a function of frequency.

The displacement Δ of the polyurethane film of 50 μm thick was also measured as a function of driving field at 100 Hz and the result is shown in figure 20. As expected, the displacement exhibits a V^2 dependence where V is the applied voltage. Clearly, the result demonstrates that at this frequency, the set-up has a resolution much below 10^{-2} Å for a soft thin polymer film.

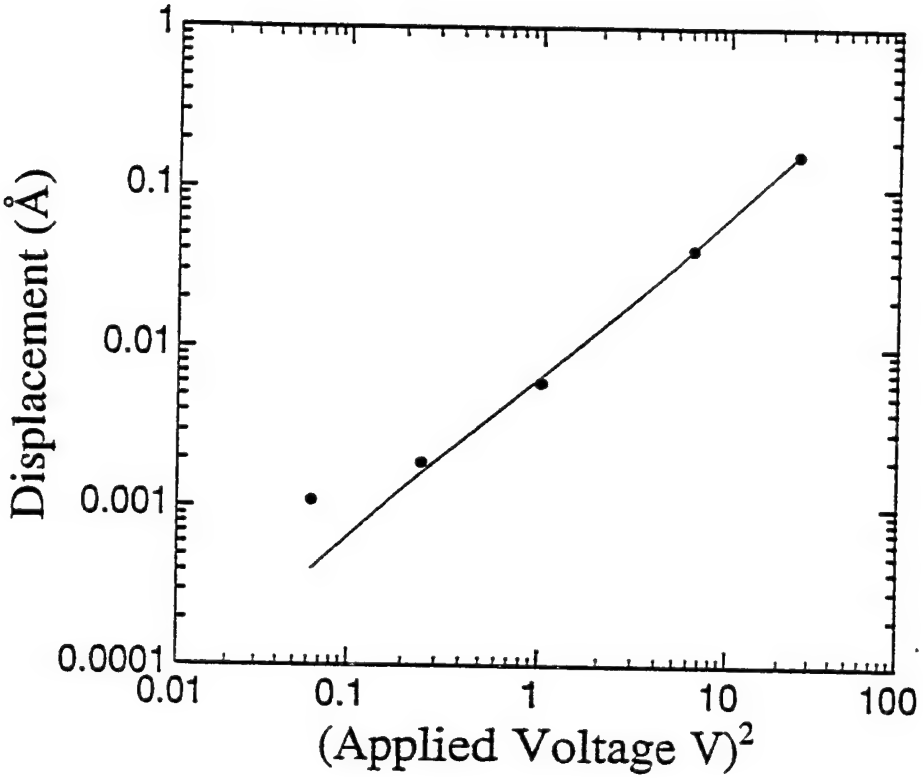

Figure 20. The displacement measured from a polyurethane thin film (50 μm) under an electric field of 100 Hz as a function of applied voltage. The black dots are the data and solid line is a fitting: Displacement -- V^2. The data demonstrate the high resolution of the system (much below 0.01 Å).

IV. Thickness Dependence of the Electric Field Induced Strain Response and Space Charge Enhanced Strain Response in Thin Film Samples

In this investigation, we found (as has been shown in figure 18) that the electric field induced strain response of the polyurethane elastomers exhibits a strong thickness dependence. As shown in figure 21(a), with a fixed field, the strain S_3, which is measured in the direction parallel to the applied electric field E, of a 0.1 mm thin film is much higher than that in a 2 mm thick sample

although the strain-field relationship in both samples follows $S_3=R\ E^2$, where R is the strain coefficient. Data presented in figure 21(b) summarizes this thickness dependence behavior. Since the elastic compliance of the polymer is much higher than that of the gold electrode, the electrodes impose mechanical clamping on the polymer and reduce the measured strain response, especially in thin film samples.[30] In the figure, the data for the corrected strain response, which takes the

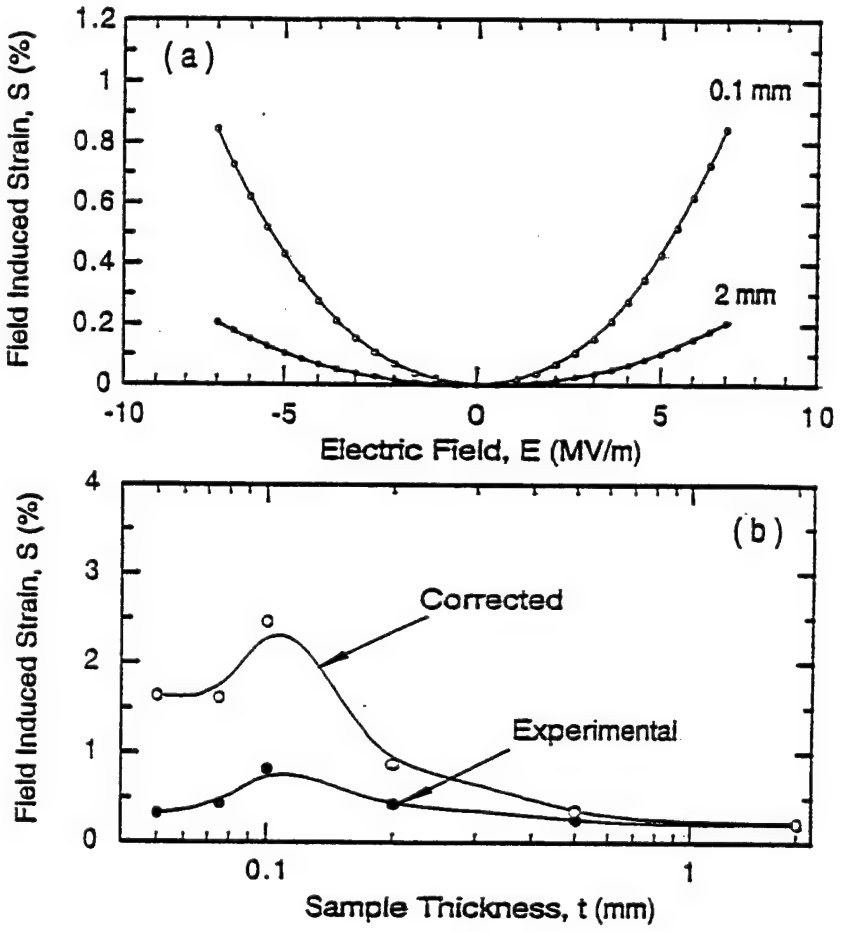

Figure 21. (a) Comparison of the strain response, measured at 2 Hz, from a 0.1 mm thick and 2 mm polyurethane samples (Dow 2103-80AE). (b) The thickness dependence of the strain response in polyurethane elastomers (measured at 2 Hz). The black dots are the measured data and the open circles are those after the correction for the gold electrode mechanical clamping effect. Solid lines are drawn to guide eyes.

electrode clamping effect into consideration, are also shown. Apparently, the high strain sensitivity of the material reported is a thin film effect and in thick samples, the strain sensitivity of the material is not very high. In addition, the frequency dispersion of a 0.1 mm film is also much stronger than that from a 2 mm thick sample as presented in figure 22.

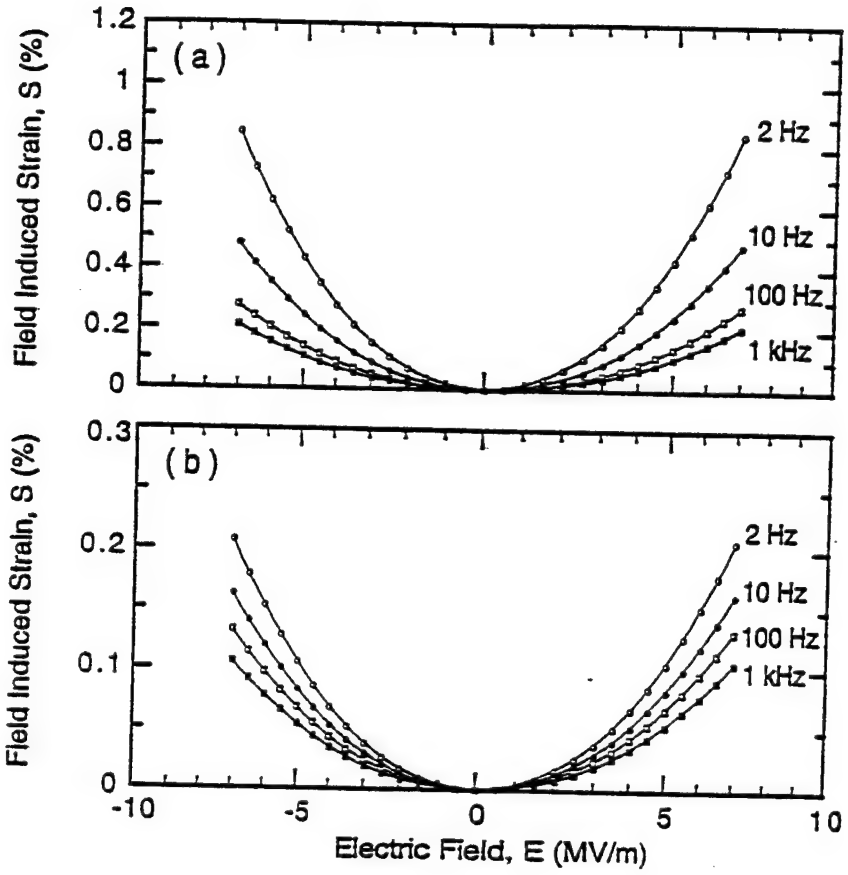

Figure 22. Frequency dispersion of the strain response of (a) 0.1 mm thick sample, and (b) 2 mm thick sample, respectively. The frequency dispersion of 2 mm thick sample is much smaller than that of 0.1 mm thick sample.

All the samples used in this investigation were made by the solution casting method from Dow 2103-80AE polyurethane. The electrodes were sputtered gold film of 300 Å thick. The strain measurement was made with a high sensitivity bimorph cantilever based dilatometer as described in the preceding section.

In searching for possible mechanisms for the large strain response in thin polyurethane films, we note that the dielectric constant and elastic compliance of the material do not show much change with thickness and their frequency dispersions are also much weaker than the strain dispersion from a 0.1 mm thick film. The observed thickness and frequency dependence of the strain response, hence, indicate the existence of other factors contributing to the high strain sensitivity in thin films and it is likely to be related to the electrode-polymer interface effects. In insulating polymers, one of the most commonly observed interface effects is the charge injection under external fields.[31,32] These charges can be from electrons and holes injected from the electrodes and/or impurity ions in the samples, and can be trapped in the interface and interphase regions, as well as other defect sites, resulting in a non-uniform space charge distribution which usually has a strong thickness and frequency dependence.

In order to investigate this possibility, samples were made from filtered solution (using a Fisher-P5 filter) in an attempt to remove some of the impurities from the original material. As shown in figure 23(a), there is a significant reduction in the strain response in the filtered films, where the data were from films of 0.1 mm thick. While in thick samples, there is not much difference in the strain response in filtered and non-filtered samples. Correspondingly, the thickness dependence of the strain response in the filtered samples is significantly reduced. Accompanying the strain reduction, the frequency dispersion of the strain response in filtered samples of 0.1 mm thickness also becomes nearly the same as that of a 2 mm thick sample as illustrated in figure 23(b).

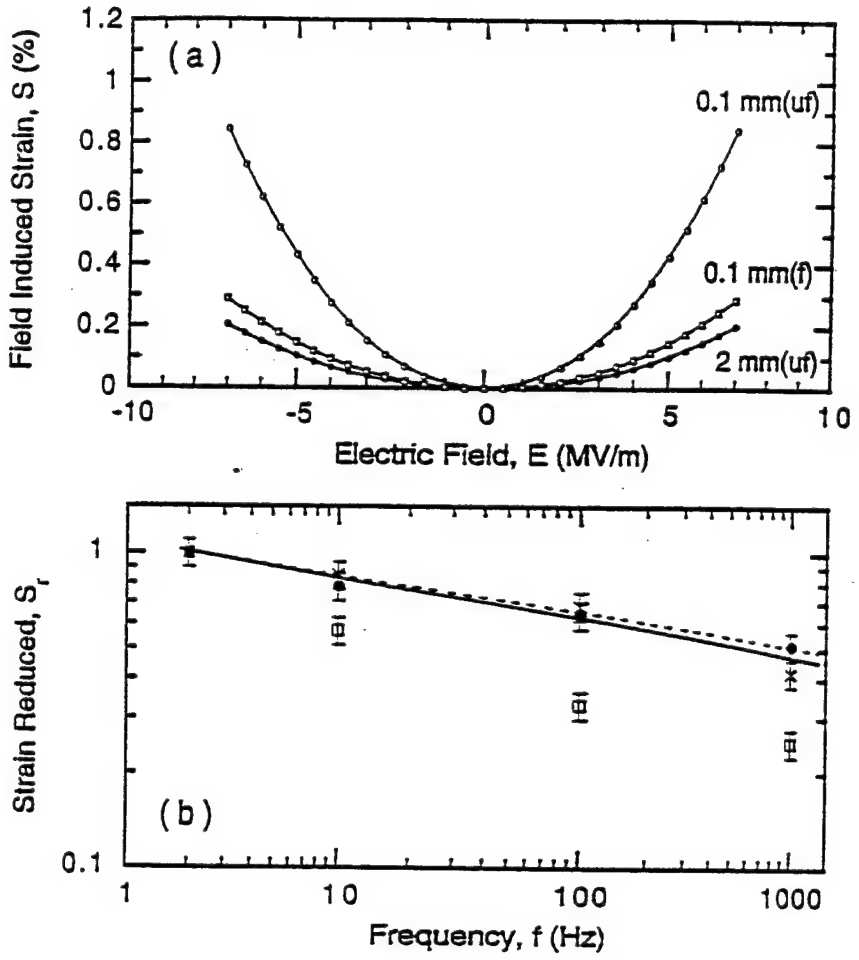

Figure 23. (a) Comparison of the strain response of unfiltered sample (uf) of 0.1 mm thick, filtered sample of 0.1 mm thick (f), and sample of 2 mm thick. For the 2 mm thick sample, there is very little difference in the strain responses between the filtered and unfiltered samples. (b) Comparison of the frequency dispersion of unfiltered sample of 0.1 mm thick (open squares), filtered sample of 0.1 mm thick (crosses), and 2 mm thick sample (black dots). The solid lines are drawn to guide eyes.

The thermally stimulated discharge current (TSDC) method, a technique widely used to characterize the charge injection in polymeric materials, was employed to study the charge injection in these samples.[33] In this method, a sample was subjected a high DC electric field (E= 4 MV/m) at a high temperature (here at 80 °C) for 5 minutes, and then cooled down under the field

to a low temperature (here at -70 °C). TSDC data were collected for both non-filtered and filtered films where the samples were heated at 4 °C/min without external bias field.

As presented in figure 24, for non-filtered sample, there are four significant peaks in the temperature range measured. By comparison with the dielectric constant data, it can be identified that the peak 1 (at -35 °C) and peak 3 (at 45 °C) are related to the glass transition of the soft segments and "glass transition" in the hard segments, respectively. Both peaks are followed by a discharge peak, i.e., peak 2 (near 10 °C) and peak 4 (near 70 °C).[34,35] In analog to other polymer systems, these discharge peaks can be identified as related to the non-uniformly distributed space charges in the soft segment region and the hard segment region, respectively. Hence, TSDC data confirm the existence of the non-uniform space change formation due to charge injection.

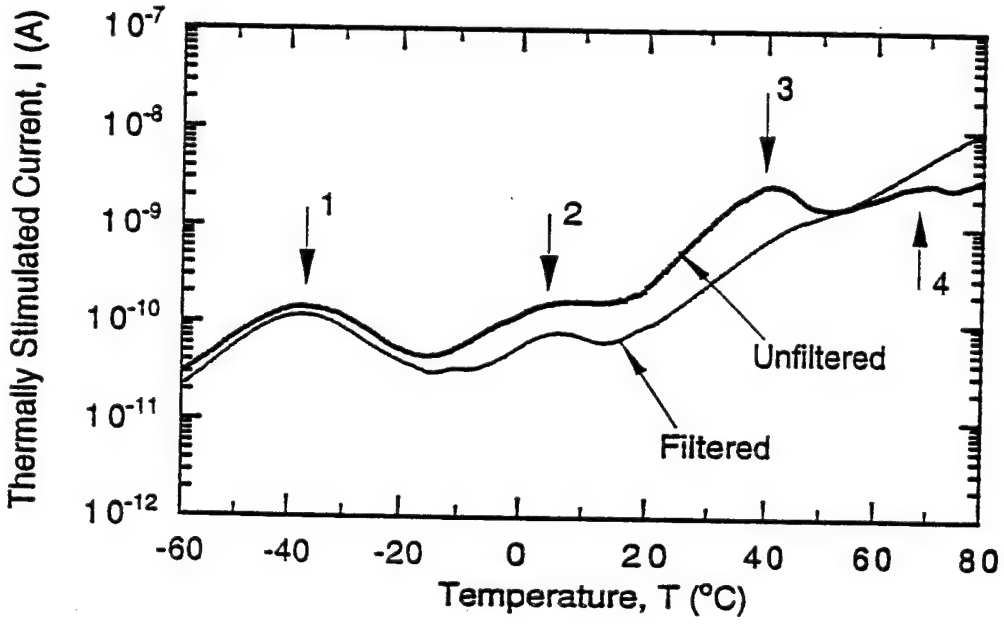

Figure 24. Thermally stimulated current data for both unfiltered and filtered samples. The thickness of the samples is 0.1 mm and area is about 1.2 cm^2.

When the curve of the filtered film is examined, it is clear that there are marked changes in the TSDC data between the non-filtered and filtered samples. Although the peak related to the glass

transition of the soft segments does not show much change, the peak area underneath the peak 2 is reduced by about half, indicating a reduction of the trapped space charges in the filtered sample in the interface region. In addition, the peak 3 is significantly reduced while the following discharging peak becomes barely visible. These results imply that the contributors which can trap the space charges to form a non-uniform space charge distribution in the sample have been significantly reduced by filtering.[36,37] Since the mesoscopic morphology of a polyurethane elastomer consists of hard segments embedded in a soft segment matrix, the interfaces between the soft segment and hard segment will act as space charge trapping sites. The change in the hard segments as revealed by the change in the peak 3 due to the filtering will likely change the energy levels at these trap sites and hence, the trap modulated space charge mobility and charge injection process.[35,38,39]

Based on these results, we suggest that the enhanced strain response in thin polyurethane films is a consequence of the change injection which results in a non-uniform space charge distribution across the thickness direction. From the Poisson's equation, it can be deduced that such a charge distribution will produce a non-uniform local electric field across the thickness direction, especially in the electrode-polymer interface.[36] Hence, the effect is not significant in thick samples. For the polymer studied here, the electric field induced strain locally S(x) is proportional to the square of the local field E(x) and hence, the total strain response S of the sample is equal to

$$S = \frac{1}{t}\int_0^t S(x)dx = \frac{R}{t}\int_0^t E^2(x)dx$$

where we have assumed the strain coefficient R is nearly a constant in the sample. t is the sample thickness. It can be shown that for a fixed applied voltage $V = \int_0^t E(x)dx$, $\int_0^t E^2(x)dx > (\int_0^t E(x)dx)^2 / t$. That is, any non-uniform field distribution across the thickness direction will enhance the strain response if the coupling between the strain and electric field is

through a square relationship such as the electrostriction and Maxwell stress effect. In fact, such an enhancement mechanism can also be generalized to other effects such as Kerr electro-optical effect to improve the sensitivity. In this scenario, in thick samples, the local electric field is not very different from the average field and there is no enhancement effect due to the interface space charge. As the film thickness is reduced, the local field becomes much higher than the average field, resulting in an enhanced electromechanical response. In an even thinner films where the two interface regions near the two electrodes start to overlap which reduces the non-uniform charge distribution, this enhancement effect is reduced as shown in figure 21.

V. Summary

Polyurethane elastomer (Dow 2103-80AE) has been investigated on its application for the acoustic transducetions. It was found that the large electric field induced strain response reported earlier is only a thin film effect. In thick samples, the field induced strain is not very large. In order to provide understanding on the electromechanical response in the materials, both the bulk samples and thin films were examined.

For the bulk sample, it was found that the Maxwell stress contribution to the strain response can be significant at temperatures higher than the glass transition temperature. In addition, the material also exhibits a very large electrostrictive coefficient Q, about two orders of magnitude higher than that of PVDF. It was also found that the Q shows little change in the glass transition temperature region while the elastic compliance changes by more than one order magnitude. On the other hand, in the second transition temperature region (the glass transition of the soft segment), the Q exhibits increase with temperature, indicating a change in the polarization behavior in the material.

The experimental results also show that for the polyurethane elastomer investigated, the temperature frequency superposition principle can be applied to both the dielectric and elastic

data, while the change of the electrostrictive coefficient with temperature and frequency does follow this superposition principle. It was also found that in a polymeric material, the chain segment motions can be divided into those related to the polarization response and those related to the mechanical response. The overlap region between the two yields the electromechanical response of the material. In general, the activation energies for the two types of motions can be different which results in different relaxation times observed in the dielectric data, elastic compliance data, and the electrostrictive data, as observed in the polyurethane elastomer investigated. The higher glass transition temperature from the mechanical data and the decrease of the Q with frequency indicate that in the temperature investigated, the activation energy for the mechanical related segment motions is higher than that of non-mechanical related segment motions. This discovery indicates the a material with a high electromechanical response can be engineered to have dielectric and mechanical properties adjustable over a wide range, a feature highly desirable for underwater acoustic applications. The experimental results also indicate the importance of the transition phenomena on the electrostriction since it can change the response behavior of polymer chains.

In order to understand how the observed macroscopic properties are related to the molecular structure, DSC, FTIR, and thermal expansion measurement were also carried out in the corresponding temperature range. The results suggest that the second transition observed at temperatures near 70 °C is related to the molecular motion of the extenders within the hard segments.

In order to study the electric field induced strain response, a novel bimorph based dilatometer was developed which can measure the strain response in thin and soft polymer films reliably and conveniently. The test results demonstrated that this device is capable of detecting displacement below 0.01 Å at 100 Hz.

Making use of this newly developed dilatometer, we studied the thickness dependence of the field induced strain in the polyurethane down to 20 μm. Based on the frequency dispersion of the

strain response in samples with different thickness and the thermally stimulated discharge current on samples with different processing conditions, we suggest that the charge injection, an interface effect, which results in a non-uniform space charge distribution and, hence, a nonuniform electric-field distribution across the sample thickness, is responsible for the large electric field induced strain response observed in thin polyurethane samples.

References:

1. W. G. Cady, "Piezoelectricity" (Dover Publications, Inc., New York 1964).

2. J. M. Herbert, "Ferroelectric Transducers and Sensors" (Gordon and Breach Science Publishes, N. Y. 1982).

3. B. Jaffe, W. R. Cook, Jr., and H. Jaffe, "Piezoelectric Ceramics" (Academic Press, London and N. Y. 1971).

4. A. J. Lovinger, Science 220, 1115-1121 (1983).

5. H. R. Gallantree, IEE Proceedings 130, 219-224 (1983).

6. H. Wang, Ph. D. Thesis, The Pennsylvania State University (1994).

7. M. Zhenyi, J. I. Scheinbeim, J. W. Lee, and B. A. Newman, J. Polym. Sci. Part B: Polym. Phys. 32, 2721 (1994).

8. I. Ladabaum, B. T. Khuri-Yakub, D. Spoliansky, Appl. Phys. Lett. 68, 7 (1996).

9. N. G. McCrum, B. E. Read, and G. Williams, "Anelastic and Dielectric Effects in Polymeric Solids" (Dover Publications, Inc. New York 1967).

10. G.M. Sessler, editor, "Electrets" (Springer-Verlag, Berlin Heidelberg 1987).

11. P. Wright and A. P. C. Cumming, "Solid Polyurethane Elastomers" (Gordon and Breach Sci. Pub., N. Y. 1969).

12. Q. M. Zhang, S. J. Jang, and L. E. Cross, J. Appl. Phys. 65, 2807 (1989).

13. Y. Tada, Jpn. J. Appl. Phys. 34, 1595 (1995).

14. V. Sundar and R. E. Newnham, Ferro. 135, 431 (1992).

15. J. Zhao, Q. M. Zhang, N. Kim, and T. Shrout, Jpn. J. Appl. Phys. 34, 5658 (1995).

16. E. A. McLaughlin, J. Powers, M. B. Moffett, and R. S. Janus, data presented at 1996 ONR Review on Transducer and Transducer Materials, The Pennsylvania State University (1996).

17. M. Haun, Ph. D. Thesis, The Pennsylvania State University (1983).

18. T. Furukawa and N. Seo, Jpn. J. Appl. Phys. 29, 675 (1990).

19. V. W. Srichatrapimuk and S. L. Cooper, J. Macromol. Sci.-Phys., B15(2), 267 (1978).

20. N. R. Legge, G. Holden, and H. E. Schreoder, "Thermoplastic Elastomers: A Comprehensive Review", (Hanser Publishers, Munich, Vienna and New York, 1993).

21. W. J. Macknight and M. Yang, J. Polym. Sci.: Symposium, 42, 817 (1973).

22. R. W. Seymour and S. L. Cooper, Macromolecules, 6, 48 (1973).

23. Ravi F. Saraf, Ho-ming Tong, Tze W. Poon, B. David Silverman, Paul. S. Ho, and Angelo R. Rossi, J. Appl. Polym. Sci. 46, 1329 (1992).

24. H. Wang, Q. M. Zhang, L. E. Cross, R. Ting, C. Coughlin, and K. Rittenmyer, Proc. Int. Symp. Appl. Ferro. 9, 182 (1994).

25. G. L. Miller, J. E. Griffith, E. R. Wagner, and D. A. Grigg, Rev. Sci. Inst. 62, 705 (1991).

26. T. Itoh and T. Suga, J. Vac. Sci. Technol. B12, 1581 (1994).

27. PZT-4 is the trademark of Morgan Matroc Inc. OH for its piezoceramic.

28. J. M. Herbert, "Ferroelectric Transducers and Sensors" (Gordon and Breach Science Publishes, N. Y. 1982).

29. Landau and E. M. Lifshitz, "Theory of Elasticity" (Oxford: Pergamon Press 1986).

30. H. Wang, Q. M. Zhang, L. E. Cross, and A. O. Sykes, Ferro. 150, 255 (1993).

31. G. M Sessler, Ed, "Electrets", Topic in Appl. Phys., Vol. 33, (Springer-Verlag, Berlin 1980) Chap. 2.

32. W. Suzuoki, H. Muto, T. Mizutami, and M. Ieda, J. Phys. D: Appl. Phys. 18, 2293 (1985).

33. J. van Turnhout, "Thermally Stimulated Discharge of Polymer Electrets", (Elsevier Sci. Publishing Comp., Amsterdam 1975).

34. E. J. Kim and Y. Ohki, IEEE Trans. on Diel. and Elect. Insulation, 2, 74 (1995).

35. A. Thielen, E. Hendrick, J. Niezette, J. Vanderschueren, and G. Feyder, J. Appl. Phys. 75, 4069 (1994).

36. K. S. Suh, D. Damon, and J. Tanaka, IEEE Trans. on Diel. and Elect. Insulation, 2, 1 (1995).

37. Y. Li, T. Takada, H. Miyata, and T. Niwa, J. Appl. Phys. 74, 2725 (1993).

38. M. M. Perlman and A. Kumar, J. Appl. Phys. 72, 5265 (1992).

39. A. Hirao, H. Nishizawa, and M. Sugiuchi, J. Appl. Phys. 74, 1083 (1993).